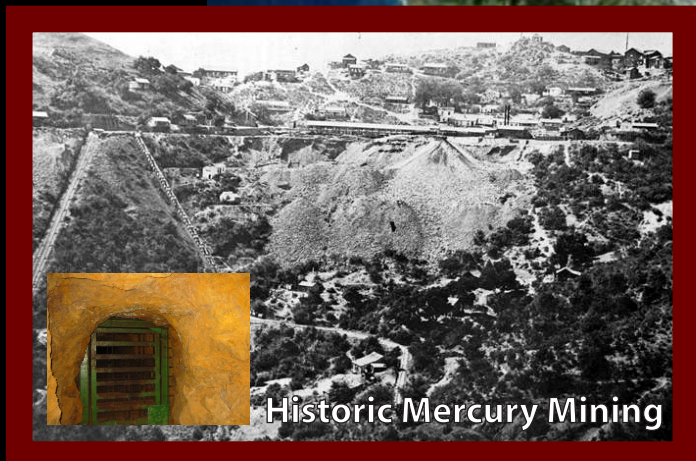


# Sediment Remobilization of Mercury in South San Francisco Bay, California

U.S. GEOLOGICAL SURVEY  
Scientific Investigations Report 2004-5196



**Cover Graphics:** A non-metallic sampling device (upper right insert) was used to collect sediment cores from South San Francisco Bay, down gradient of historic mercury mining (bottom left insert from Lanyon and Bulmore, 1967), for incubation experiments to measure the flux of dissolved-mercury species across the sediment-water interface.



# **Sediment Remobilization of Mercury in South San Francisco Bay, California**

---

**U.S. GEOLOGICAL SURVEY**

**Scientific Investigations Report 2004-5196**

# Sediment Remobilization of Mercury in South San Francisco Bay, California

By Brent R. Topping<sup>1</sup>, James S. Kuwabara<sup>2</sup>, Mark C. Marvin-DiPasquale<sup>3</sup>, Jennifer L. Agee<sup>4</sup>, Le H. Kieu<sup>5</sup>, John R. Flanders<sup>6</sup>, Francis Parchaso<sup>7</sup>, Stephen W. Hager<sup>8</sup>, Cary B. Lopez<sup>9</sup>, and David P. Krabbenhoft<sup>10</sup>

---

U.S. GEOLOGICAL SURVEY

Scientific Investigations Report 2004-5196

- <sup>1</sup> [btopping@usgs.gov](mailto:btopping@usgs.gov), U.S. Geological Survey, Menlo Park, CA
- <sup>2</sup> [kuwabara@usgs.gov](mailto:kuwabara@usgs.gov), U.S. Geological Survey, Menlo Park, CA
- <sup>3</sup> [mmarvin@usgs.gov](mailto:mmarvin@usgs.gov), U.S. Geological Survey, Menlo Park, CA
- <sup>4</sup> [jlagee@usgs.gov](mailto:jlagee@usgs.gov), U.S. Geological Survey, Menlo Park, CA
- <sup>5</sup> [lhkieu@usgs.gov](mailto:lhkieu@usgs.gov), U.S. Geological Survey, Menlo Park, CA
- <sup>6</sup> [jflander@usgs.gov](mailto:jflander@usgs.gov), U.S. Geological Survey, Menlo Park, CA
- <sup>7</sup> [parchaso@usgs.gov](mailto:parchaso@usgs.gov), U.S. Geological Survey, Menlo Park, CA
- <sup>8</sup> [swhager@usgs.gov](mailto:swhager@usgs.gov), U.S. Geological Survey, Menlo Park, CA
- <sup>9</sup> [cblopez@usgs.gov](mailto:cblopez@usgs.gov), U.S. Geological Survey, Menlo Park, CA
- <sup>10</sup> [dpkrabbe@usgs.gov](mailto:dpkrabbe@usgs.gov), U.S. Geological Survey, Middleton, WI

U.S. DEPARTMENT OF THE INTERIOR  
GALE A. NORTON, Secretary

U.S. GEOLOGICAL SURVEY  
CHARLES G. GROAT, Director

---

For additional information, contact:

Brent R. Topping

U.S. Geological Survey

345 Middlefield Road, MS 439  
Menlo Park, CA 94025

Copies of this report may be  
obtained from the authors or

U.S. Geological Survey  
Information Center  
Box 25286, MS 517  
Denver Federal Center  
Denver, CO 80225

## TABLE OF CONTENTS

Executive Summary .....	5
Physical and Biological Characterizations.....	5
Chemical Characterizations .....	6
Remedial Implications .....	7
Background.....	8
Results and Discussion .....	10
Physical Data .....	10
Biological Data .....	10
Chemical Data.....	11
Study Design and Methods .....	18
Coring Operation .....	18
Core Incubations .....	18
Physical Data .....	19
Biological Data .....	19
Chemical Parameters .....	19
References Cited.....	22
Acknowledgments.....	27
Appendix 1: Comments on the Report Structure.....	28
Appendix 2: List of Figures .....	29
Appendix 3: List of Tables .....	30

# Sediment Remobilization of Mercury in South San Francisco Bay, California

By Brent R. Topping, James S. Kuwabara, Mark C. Marvin-DiPasquale, Jennifer L. Agee, Le H. Kieu, John R. Flanders, Francis Parchaso, Stephen W. Hager, Cary B. Lopez and David P. Krabbenhoft

## Executive Summary

Field and laboratory studies were conducted in April and November 2003 to provide the first direct measurements of the benthic flux of dissolved (0.2-micrometer filtered) mercury species (total and methylated forms) between the bottom sediment and water column at two sampling locations within the southern component of San Francisco Bay, California (hereafter referred to as South Bay): one within the main channel and the other in the western shoal area ([Fig. 1](#)). Because of interest in the effects of historic mercury mining ([Fig. 2](#)) within watersheds that drain into South Bay, the solutes of primary interest were dissolved-mercury species and the predominant ligands that often control mercury speciation (dissolved sulfide and dissolved organic carbon). Benthic flux, sometimes referred to as internal recycling, is the transport of dissolved chemical species between the water column and the underlying sediment. Because of the affinity of mercury to adsorb onto particle surfaces and to form insoluble precipitates (particularly with sulfides), the mass transport of mercury in mining-affected watersheds is typically dominated by particles. As these enriched particles accumulate at depositional sites such as estuaries and reservoirs, benthic processes facilitate the repartitioning, transformation, and transport of mercury in dissolved, biologically reactive forms (dissolved methyl-mercury being the most bioavailable for trophic transfer). These are the forms of mercury examined in this study.

During two sampling events, three replicate sediment cores ([Coring methods; Fig. 3](#)) from each of two South Bay locations (Station 29A, a deep, main-channel site; and Station 25, a western shoal site; [Fig. 1](#)) were used in incubation experiments to provide flux estimates and benthic biological characterizations. Incubation of these cores provided “snapshots” of solute flux across the sediment-water interface in this component of the estuary, under environmental conditions representative of the time and place of collection. Ancillary data, including nutrient and ligand fluxes, were gathered to provide a water-quality framework from which to compare the results for mercury. The following major observations from interdependent physical, biological, and chemical data were made:

### Physical and Biological Characterizations

1. **Porosity:** The surficial sediment at Station 29A was generally of higher porosity than that at Station 25 on both sampling dates. Station 29A porosities ranged from 0.77 to 0.92 ( $0.84 \pm 0.05$ ), while those of Station 25 ranged from 0.73 to 0.82 ( $0.77 \pm 0.04$ ). This difference, however, is not statistically significant at the 95% confidence interval.
2. **Benthic Biota:** Macroinvertebrate densities varied temporally and spatially ([Table 1](#)), in a manner consistent with previous studies (Topping and others, 2001; see [macroinvertebrate discussion](#)). Given that the first sampling event coincided with the annual spring phytoplankton bloom in the South Bay, Chlorophyll and phaeophytin concentrations ([Table 2](#)) also exhibited temporal and spatial differences. See the [results](#) section for details.

## Chemical Characterizations

Note: The dissolved-mercury concentrations discussed in this section refer to samples filtered with 0.7-micrometer quartz-fiber filters pre-combusted at 500 °C for 12 hours.

- 1. Dissolved mercury in the water column:** Dissolved methyl-mercury concentrations were below detection limits at all sites and dates. Total dissolved-mercury concentrations ranged from ~4 to ~10 picomolar, so the undetectable methyl-mercury values were not surprising because total mercury concentrations are typically two or more orders of magnitude greater than methyl-mercury concentrations. Total dissolved-mercury concentrations were appreciably elevated at the western-shoal Station 25 relative to the main-channel Station 29A, and in spring relative to autumn. ([Table 3](#), [Mercury results](#)).
- 2. Benthic flux of dissolved forms of mercury:** When the three cores for each site were averaged, benthic flux estimates for total dissolved-mercury showed no temporal change for Station 25, but showed higher flux in spring relative to fall for Station 29A ([Table 4](#)). Still, the averages for each site and date were within the same order of magnitude. When the average for all sites and dates ( $135 \pm 94$  g/day; [Table 4](#)) is extrapolated over the greater South Bay, the magnitude of the values is consistently comparable to or greater in magnitude than estimates of major riverine sources ([Fig. 4](#)). Notably, benthic flux of dissolved mercury is of the same magnitude as particulate mercury inputs from the Guadalupe River watershed ( $318 \pm 88$  g/day in 2003; McKee 2004, draft copy). Transport of dissolved-mercury species between the estuary bed and water column may therefore be a potentially critical process regulating the fate of mercury species in the water column ([Mercury flux discussion](#)).

All twelve individual core incubations in the study resulted in positive total-mercury flux values ([Table 4](#)). In other words, at all sites and dates, each core indicated that dissolved total mercury was transported out of the sediment into the overlying water column.

Dissolved methyl-mercury fluxes could not be directly calculated due to the undetectable values for all sites and dates (<0.5 picomolar in May, <0.2 picomolar in November). These undetectable values are common and have been observed in other studies (Conaway and others, 2003). However, when comparing loads of dissolved methyl-mercury into South Bay, benthic flux cannot be summarily discounted as a possible source due to analytical limitations ([Load comparison discussion](#)).

Ancillary measurements characterizing the sediment were compared with water-column and benthic flux values. Four correlations were observed including sediment mercury's correlation with benthic flux of dissolved mercury ([Ancillary sediment characterization discussion](#)).

### **3. Benthic flux of mercury-binding ligands:**

Dissolved-sulfide benthic fluxes were similar at all dates and sites ([Table 5](#)), and consistently positive. Sulfides are associated with reducing conditions, so the similarities at all stations and dates might indicate reducing-oxidizing (redox) conditions were similar throughout the study, despite significantly higher dissolved oxygen (DO) consumption in May ([DO discussion](#)). Given that the South Bay water column is consistently oxic (that is, dissolved-sulfide species are only metastable), the relative consistency of the mercury fluxes may be associated with the flux of sulfides, which have a strong affinity to complex with mercury.

Dissolved organic carbon (DOC) fluxes were markedly different between sites and significantly so between dates ([Table 6](#); [Fig. 5](#)). Autumn fluxes were much higher than spring fluxes at both sites,

while Station 29A exhibited higher fluxes than Station 25 for both dates. Unlike sulfides, negative DOC fluxes (solute transport from the water column to the bottom sediment) were observed in some cores.

#### **4. Benthic flux of other metals:**

Comparisons between this study and a previous one by the authors (Topping and others, 2001) indicated that 2003 conditions may be less conducive to metal remobilization and release than in previous years ([Dissolved nickel and copper discussion](#)). This indicates that estimates of long-term mercury flux could be incorrectly low if based only on 2003 sampling.

### Upgradient Remedial Implications

Because the benthic flux of mercury appears to represent a dominant transport process for dissolved, more bioavailable forms, an important management implication is suggested. Remediation efforts and Total Maximum Daily Load (TMDL) allocations along the Guadalupe River have dual objectives of decreasing concentrations and loads to down-gradient systems in an effort to reduce bioaccumulation of mercury in fish consumed by humans and wildlife. Using preliminary mercury-flux estimates into the estuary, our results indicate that a significant (and possibly predominant) percentage of dissolved mercury in the water column presently comes from the bay sediment ([Mercury flux discussion](#)). If upstream sources are controlled, which is desirable even apart from estuary effects, the change in inflow loads is likely to be compensated in part by increases in benthic flux ([Fig. 6](#)).

### Comment on the Report Structure

In contrast to typical scientific manuscripts, this report is formatted in a pyramid-like structure to serve the needs of diverse groups who may be interested in reviewing or acquiring information at various levels of technical detail ([Appendix 1](#)). The report enables quick transitions between the initial [summary information](#) (figuratively at the top of the pyramid) and the later details of [methods](#) or [results](#) (figuratively towards the base of the pyramid) using hyperlinks to supporting figures and tables, and an electronically linked [Table of Contents](#).

## Background

South San Francisco Bay and the Guadalupe River watershed represent a CERCLA (Comprehensive Environmental Response Compensation and Liability Act) site affected by drainage from the New Almaden mines. Mercury at the New Almaden mines, and more generally in California coastal ranges, was hydrothermally deposited under silica carbonate formations during the Cenozoic Era (Rytuba and Enderlin, 1999). These cinnabar (mercury sulfide) ores were mined, heat-processed and distilled to acquire elemental mercury. The mines, a National Historic Landmark since 1975, are historically significant on many spatial scales. In full operation by 1850, it was the first large-scale mining operation in California. The New Almaden mines are the most productive mercury mines in the history of the United States with total production exceeding 30 million kilograms of elemental mercury. Globally, discovery of and production from this location, fortuitously timed just prior to the California gold rush (Alpers and Hunerlach, 2000), freed the United States from an existing monopoly of the mercury market by the House of Rothschild in England (Goss, 1958; Johnson, 1963; Lanyon and Bulmore, 1967; Schneider, 1992). Acknowledging these important economic contributions to the burgeoning state, the New Almaden mines also leave a troublesome legacy. Notably, 600,000 m<sup>3</sup> of calcine (heat-processed cinnabar) now resides within the freshwater and estuarine aquatic systems of the Santa Clara Valley watersheds. This legacy provides many reasons to suspect that sediment-water interactions significantly affect the geochemical and biological distributions of mercury in South San Francisco Bay.

Many fundamental processes affect the transport of dissolved-chemical species (for example, nutrients, metals, ligands) through and within aquatic systems. A conceptual model of these processes (Fig. 7) illustrates some physically based processes that have been examined and carefully quantified in a number of previous studies (for example, advective transport and point source inputs; Fischer and others, 1979).

There are, however, terms in the conceptual model that have until recently received little attention. A prime example is the benthic flux term. No direct measurements for dissolved-mercury species have heretofore been available for the study area, or for adjacent areas currently beginning extensive wetland-restoration of former salt ponds (website: <http://www.southbayrestoration.org/>). Benthic flux (sometimes referred to as internal recycling) represents the transport of dissolved chemical species between the water column and the underlying sediment. Flux of solutes can be either positive (into the water column from the sediment or atmosphere) or negative (out of the water column into the sediment or atmosphere) and can vary over multiple temporal and spatial scales (Kuwabara and others, 2002; Kuwabara and others, 2003a).

As a result of physical, chemical, and biological processes operating near the sediment-water interface, geochemical gradients take on a variety of forms that have been previously reported (Kuwabara and others, 2000; Fig. 6). Associated gradients in solute concentrations can thereby result in a benthic flux of that solute that may be **negative or consumed by the sediment, positive or released from the sediment**, or insignificant when the gradient is indistinguishable. When interdependent factors regulate the benthic flux of biologically reactive substances, the vertical gradient for one dissolved species may be dependent on the gradient of another chemical species. For example, an **attenuated release** may occur when solute concentrations increase below the sediment-water interface only when another solute is depleted. Redox-sensitive solutes like dissolved iron often behave in this manner when suboxic conditions reduce it from ferric (Fe<sup>+3</sup>) to ferrous (Fe<sup>+2</sup>) forms, increasing its solubility and releasing adsorbates. Macrofauna can also enhance benthic flux by irrigating or disturbing surficial sediment layers (**bioirrigation, bioturbation**, or biologically enhanced **advection**). Certain productive benthic communities can enhance benthic flux by orders of magnitude beyond diffusive-control (Kuwabara and others, 1999a, Thibodeaux and Bierman, 2003), while other communities are too sparse to generate this magnitude of enhancement (Kuwabara and others, 2003b). Therefore, vertical chemical gradients generated by a variety of interdependent biogeochemical processes can induce the transport of dissolved-mercury species across the sediment-water interface in estuarine systems.

Scientists and water-quality managers are only beginning to understand the importance of benthic flux in many aquatic environments. Within the past decade or two, researchers have gradually realized that there are non-hydrologic processes (for example, benthic flux) that must be incorporated into water-quality models in order to generate physically meaningful information. Unfortunately, benthic-flux determinations are instrument and manpower intensive, because each flux estimate requires complex sample collection procedures and a concentration time-series analysis or vertical-profile analysis. Benthic-flux studies have consequently lagged behind studies of

other transport processes, but are spurring interest in both the scientific and management communities (Kuwabara and others, 2003b).

Water-quality managers often assess and prioritize remediation strategies for aquatic systems that have been adversely affected by anthropogenic activities. In the case of South San Francisco Bay, directly down gradient of the Guadalupe River, mercury associated with decades of productive mining at the historic New Almaden Quicksilver Mine has been fluvially transported and accumulated in the bottom sediments. Frequent demands have been made by regional managers and the public to quantify the connections between fluxes of contaminants and the health, abundance, and distribution of biological resources (Kuwabara and others, 1999a). As part of ongoing efforts to examine processes affecting trace-contaminant transport in San Francisco Bay, this study focuses on a poorly understood, yet potentially predominant, source of mercury to the estuary's water column: internal recycling, or benthic flux of mercury species and associated ligands. Mobilization, flux, and biological availability of mercury into the water column are affected by physical (for example, advection and diffusion), chemical (that is, oxidation-reduction reactions, complexation and repartitioning) and biological processes (for example, bioirrigation and bioturbation) (Flegal and others, 1991; Kuwabara and others, 1996; Grenz and others, 2000; Topping and others, 2001).

The results described herein followed from the integration of current project studies with information needs identified by the San Francisco Estuary Institute to provide initial determinations of dissolved total and methyl-mercury fluxes from the sediments into the water column of South San Francisco Bay. Beyond the ecological status of the system, elevated mercury concentrations in fish require consumption advisories relating to human health (<http://www.oehha.ca.gov/fish.html>). Quantifying and understanding the magnitude and variability of these fluxes is critical to the accurate assessment of contaminant sources and loads as well as to the development of appropriate water-quality models and remedial programs for this mining-affected system.

To help enable science based programmatic decisions related to water and ecosystem quality in San Francisco Bay, the purpose of this study is to quantify sources and sinks of dissolved total mercury and dissolved methyl-mercury associated with the bottom sediment within the South Bay relative to major surface-water inputs from the major tributaries. Owing to past mercury mining, fluvial inputs need to be compared quantitatively to the internal source of mercury. Also, there is a growing body of evidence from other aquatic systems that benthic flux of contaminants and nutrients is an important process to consider in developing appropriate ecosystem water-quality models (Wood and others, 1995; Rivera-Duarte and Flegal, 1997; Topping and Kuwabara, 2003). Thus, the need clearly exists for more refined conceptual and numerical models describing mercury dynamics within the South Bay.

## Results and Discussion

### Physical Data

Sediment texture and color were visually similar at both the western shoal site (Station 25) and the deep, main-channel site (Station 29A). At each site, the sediment is composed largely of fine-grained silts and clays. This sediment composition facilitates core-tube penetration and sediment-core retention. Main-channel porosities had a mean of  $0.84 \pm 0.05$ , and a range of 0.77 to 0.92. Western shoal porosities had a mean of  $0.77 \pm 0.04$ , and a range of 0.73 to 0.82. The difference in means superficially favors Station 29A, but it is not statistically significant at the 95% confidence interval shown.

### Biological Data

1. **Benthic macroinvertebrates:** In certain aquatic environments, bioturbation and bioirrigation by benthic macroinvertebrates can significantly affect the benthic flux of solutes (Charbonneau and others, 1997; Kuwabara and others, 1999a). Thus, macroinvertebrate taxonomies ([Table 1](#)) provide useful characterization of the benthic community. For example, *Corophium* sp. and *Ampelisca abdita*, which have been shown to enhance solute benthic flux by their feeding and sensing behaviors (Miller, 1984; Word, 1980), are the dominant crustaceans at both sites and dates. However, there is a scarcity of knowledge of species-specific data regarding biological effects on flux values. Aller and Aller (1998) showed how increased macroinvertebrate density led to exponentially higher flux values for manganese, but these results can't be assumed to translate to mercury or other solutes. However, Choe and others (2004) found that estimated diffusive fluxes of mercury were only a small portion of the directly measured benthic flux. Because it is difficult to quantify the effect of these biological activities, this macroinvertebrate density information only serves as a qualitative description of the benthic community's potential impact on the benthic flux of solutes.

Due to the compilation of a similar dataset in 1998/1999, which appears in Topping and others, 2001, comparisons can be made regarding long-term, as well as short-term, temporal variability. At Station 25, samples were taken in April and September, 1998, allowing for comparisons between spring and fall sampling. Paralleling 1998, Station 25 showed increases, from spring to fall, in annelid and mollusc biomass, but showed a marked decrease in crustacean biomass in 2003. Mollusc biomass fell precipitously from fall 1998 to fall 2003.

Station 29A was sampled only in May, 1999 in the previous study, so comparisons can only be made between spring dates. Total biomass of crustaceans and molluscs were similar in spring between 1999 and 2003, but annelid biomass was orders of magnitude higher in 2003.

In terms of individuals per square meter, the colloquially-named "Bamboo worm", *Sabaco elongatus*, is the most abundant macroinvertebrate in fall 2003 at both sites. It is also relatively plentiful in the spring samples. Curiously, this invasive polychaete was nearly absent from all samples in 1998/1999, despite being described as abundant at earlier dates (Nichols and Pamatmat, 1988). Conversely, notably absent from the 2003 sampling was the Asian clam *Potamocorbula amurensis*, which was relatively numerous at Station 25 in 1998.

2. **Benthic chlorophyll-*a*:** Chlorophyll-*a* (chl-*a*) concentrations in surficial sediments ranged from  $< 0.1$  up to 4.7 micrograms per square centimeter with the highest concentrations observed at the shoal site during the spring sampling, and the lowest concentrations at the main-channel site during the fall sampling ([Table 2](#)). This data coincides with the spring phytoplankton blooms, which deposits chl-*a* on the sediment as it settles gravitationally. The concentration ratio of chl-*a* to chl-*a*

plus phaeo-pigments (CCP ratio) is used as a crude indicator of the extent of senescence in an algal population (Thompson and others, 1981; Kuwabara and others, 1990). Ratios greater than 0.5 indicate active growth, and values less than 0.5 suggest enhanced pigment degradation associated with cell senescence or predation pressures that process the chlorophyll-*a* to degradation products. Predictably, the benthic CCP ratio for the spring sampling ( $0.15 \pm 0.10$ ,  $n=6$ ) was significantly higher than the fall ( $0.02 \pm 0.02$ ,  $n=6$ ). This seasonal discrepancy is typical for the South Bay due to its regular springtime phytoplankton blooms (Cloern, 1996).

## Chemical Data

For consistency with previous geochemical studies, mercury flux estimates are presented in mass-flux units, but were also tabulated in molar units.

- 1. Dissolved oxygen (DO) benthic flux:** While spatial differences were not apparent, seasonal differences were significant for dissolved oxygen consumption from the water column ([Table 7](#)). The cores taken in spring averaged a dissolved oxygen flux of  $-4.6 \pm 0.3$  millimoles per square meter per hour, while the autumn cores averaged  $-3.3 \pm 0.5$  millimoles per square meter per hour. This difference could be caused by phytoplankton respiration since the benthic chl-*a* values were higher in the spring, and the experiment was conducted in near darkness. Oxygen consumption rates for both sites were high relative to previous experiments at the same location by the authors (results unpublished). This could indicate a more active than normal bacterial population. In fact, the dissolved oxygen concentrations in the cores' overlying water were all suboxic ( $\sim 1$  mg/L dissolved oxygen) in May 2003. These levels of oxygen could alter the redox (reduction-oxidation) conditions, and may affect the flux of certain solutes from the sediment ([Mercury flux discussion](#))
- 2. Dissolved mercury in South Bay bottom waters:** (Note: Error values in this section reflect standard deviations due to low sample replication) At both sampling sites, higher dissolved total-mercury concentrations ([Table 3](#)) were observed in May relative to November. At Station 25, which was only sampled at one depth due to its shallowness, samples measured  $10.0 \pm 0.2$  picomolar in May, but only  $5.7 \pm 0.9$  picomolar in November. At Station 29A, a 3-point water-column profile was taken encompassing shallow, mid-depth, and bottom water samples. In the case of the shallow samples ( $7.0 \pm 0.1$  picomolar in May;  $4.7 \pm 0.1$  picomolar in November) and the mid-depth samples ( $6.8 \pm 0.0$  picomolar in May;  $3.8 \pm 0.1$  picomolar in November), this difference quite pronounced, as at Station 25. The bottom water samples ( $5.4 \pm 0.5$  picomolar in May;  $4.8 \pm 0.2$  picomolar in November) at Station 29A do not exhibit this seasonal difference at a statistically significant level. Conaway and others, 2003, analyzed surface-water samples for total-dissolved mercury at the three South Bay sites that are geographically near our stations. The authors observed a range in values from 0.9 to 6.8 picomolar for fourteen samples taken in 1999-2000.

Within each Station 29A profile, the vertical concentration gradient can be investigated to reveal benthic sources or sinks. In May, the lower concentrations at depth are counter-indicated with our positive mercury benthic flux data, which would suggest that bottom-water concentrations would be elevated. However, the estuary is vertically well-mixed, and any gradients established by benthic flux would not be maintained. In November, the concentration minimum was found at mid-depth, but the shallow and deep samples were very similar.

All methyl-mercury concentrations were below detection limits (reported as 0.5 picomolar in May and 0.2 picomolar in November). Conaway and others, 2003, also reported consistently low values at the aforementioned sites. Reporting a detection limit of 0.05 picomolar for dissolved methyl-mercury, the authors observed a range from  $<0.05$  to 0.4 picomolar for eight samples taken in 1999-2000.

3. **Mercury benthic flux:** In contrast to typical management strategies which focus on particulate mercury that dominates total loads to the estuary, this study focused on dissolved, more bioavailable, species. Mercury has a very high affinity for binding with particles, but the mercury remaining in solution has the potential to be bioaccumulated and biomagnified up the food chain, potentially resulting in human-health fish-consumption advisories (Abu-Saba and Tang, 2000).

Dissolved total-mercury fluxes were positive (that is, out of the bed sediment) in all six core incubations in May 2003 and all six core incubations in November 2003. Fluxes, averaged at each site/date, were greatest at Station 29A in May and lowest at the same station in November. However, site/date average fluxes were within the same order of magnitude ([Table 4](#); values are given in both molar and mass units). While the largest site/date average flux was seen at Station 29A in May, this value is driven mostly by one elevated value (Core 5). In fact, all but three of the twelve core incubations produced calculated fluxes between 18 and 54 picomoles per square meter per hour, indicating a relatively consistent flux at all times and sites. For comparison, similar studies done for mercury-impacted Sierra Nevada reservoirs (Kuwabara and others, 2002; Kuwabara and others, 2003a) produced a range of values from 80 to 1600 picomoles per square meter per hour.

Due to the elevated dissolved-oxygen consumption mentioned above ([DO discussion](#)), the final time-point (12 hours; see [Methods](#)) for all May cores was suboxic (~1 mg/L dissolved oxygen in the water overlying the sediment core). This is atypical in the South Bay, where bottom waters are predominantly near DO saturation (Cloern and others, 2003). Thus, it is possible that mercury fluxes could have been affected during the last interval of the incubations due to redox-driven dissolution or complexation dynamics. To address this concern, mercury fluxes were recalculated, excluding the final time-point in each May core, but the results were very similar to those using the entire time series ([Table 4](#)). Also, others have found that mercury fluxes appeared higher under oxic conditions than suboxic (R. Mason – personal communication, Sept. 2004).

**Load comparisons:** For purposes of comparison to loads from the Guadalupe River watershed, the South Bay flux values were converted to g/day (loading) by extrapolating these fluxes over the entire South Bay (south of the Bay Bridge) surface area (554 km<sup>2</sup>; Cheng and Gartner, 1985). Considering the relative consistency of the values, an average of all sites/dates was used for comparisons. Thus, it is estimated that 135 +/- 94 g/day of dissolved mercury fluxes into the bay from the sediment ([Table 4](#)).

Mercury concentrations and river discharges were measured in a dry-season scenario (TetraTech, 2003) within the Guadalupe River watershed. The report calculated a range of 0.1-0.3 g/day of dissolved mercury for a late-July, low-flow condition ([Fig. 4](#)). Although Hg measurements were not made during a high-flow storm in December 2002, assumptions were made based on the 3 orders of magnitude increase in flow. While particulate concentrations increase exponentially with flow, dissolved-Hg concentrations remain steady (presumably due to the balanced effects of dissolution, adsorption/desorption and dilution). Thus, if it's assumed that dissolved-mercury loads would increase in proportion to river discharge, these assumptions lead to a loading estimate of 100-300 g/day for dissolved Hg from the Guadalupe River during a high-flow event ([Fig. 4](#)). Additionally, data from Thomas and others (2002) can be used to calculate a load of 1.2 g/day of dissolved mercury during a lesser rain event in October 2000.

Based on these preliminary loading estimates, this comparison indicates that benthic flux from the sediment is likely to be a dominant source of dissolved Hg to the water-column particularly during the dry season (May-Oct). Furthermore, historic meteorological data (Goodridge, 2000) indicate

that >90% of the days in the region are without significant precipitation, suggesting that the temporal importance of benthic flux could extend well beyond the dry season. Furthermore, McKee and others (2004, draft copy) found that particulate mercury loading occurs episodically (66% in one month for the study year), and that most days do not contribute appreciably to their 113 kg/year estimate of particulate mercury loading to lower South Bay.

Since all dissolved methyl-mercury concentrations were below detection limits, no methyl-mercury fluxes could be estimated. However, calculations were made that indicate that benthic flux could still provide a source similar to, or greater than, watershed inputs for dissolved methyl-mercury. Loading estimates (TetraTech, 2003) for dissolved methyl-mercury produce a range from 0.002 to 0.005 g/day for a dry-season scenario. In order for the 12-hour core incubation to produce a flux that would extrapolate to 0.005 g/day, dissolved methyl-mercury concentrations in the incubated cores would only have needed to increase by 0.02 picograms per liter (0.0001 picomolar), which is more than 3 orders of magnitude below the detection limit. To equal a wet-season estimate (5 g/day), the concentration change would need to be 0.02 nanograms per liter, which is near the detection limit. Therefore, given the low dissolved methyl-mercury concentrations in the South Bay water column and inflowing major rivers like the Guadalupe, the analytical detection limits may mask the relative importance of the benthic flux of dissolved methyl-mercury. Although the design of our incubation experiment raises the method detection limit through volume restrictions, Conaway and others, 2003, despite lower detection limits, also couldn't observe the miniscule concentration difference required to produce a significant dry-season flux.

If management directives focus solely on the inputs of particulate mercury, the effect of such policies on mercury accumulation in fish, and other higher trophic level organisms consumed by humans, would not account for dissolved mercury contributed by benthic flux. It has been shown that sediment mercury concentrations are decoupled from bioavailability and thus bioaccumulation in organisms (Mason and Lawrence, 1999; Watras and others, 1998). Reducing all point-source inputs of Hg to the estuary may provide a very limited solution because 1) the benthic source has accumulated for over a century could remain indefinitely, and 2) even pristine aquatic environments with no point source Hg inputs (U.S. EPA, 1997) have mercury-related fish consumption advisories. Consistent with that finding, San Francisco Bay has similar advisories (Abu-Saba and Tang, 2000) despite dissolved methyl-Hg concentrations that are at times below detection limits (Conaway and others, 2003), as observed in our study. Also, Looker and Johnson (2003) estimate a long-term average load of 252 g/day of particulate mercury from the Guadalupe River watershed into the South Bay (Fig. 4), which is of the same order of magnitude as the estimate for benthic flux of dissolved mercury (135 g/day).

4. **Dissolved sulfide:** Sulfide flux was consistently positive (that is, from the sediment to the overlying water column) and ranged from 564 to 786 nanomoles per square meter per hour (average of three replicates per site per date; Table 5). At each date, the sulfide flux was appreciably higher at Station 29A, but the temporal changes are not strongly apparent at each station. These fluxes are significantly higher for two of the three matching station/season measurements done by Topping and others, 2001.

Dissolved-sulfide concentrations were below detection limits (<4 nanomolar) in the bottom water. A less sensitive method (ion-selective electrode; detection limit: 0.2 micromolar) used for porewater found detectable sulfides at only one site date: 0.58 micromolar at Station 29A in spring. Using this concentration, and assuming a 4 nanomolar bottom water concentration, a diffusive flux from the benthos was calculated with a diffusion coefficient of  $1 \times 10^{-5}$  square centimeters per second (Li and Gregory, 1974). The calculated diffusive-flux estimate was 104 nanomoles per square meter per hour, while the directly measured sulfide flux at Station 29A

([Table 5](#)) in spring averaged 751 nanomoles per square meter per hour. This large difference between a measured and a calculated flux suggest that bioturbation or bioirrigation have enhanced the flux beyond what would be expected from diffusion alone. Benthic macroinvertebrate densities have been linked to relative enhancement of benthic flux in other mining-affected aquatic systems (Caffrey and others, 1996; Kuwabara and others, 1999a; Kuwabara and others 2003a; Thibodeaux and Bierman, 2003).

Dissolved sulfide is a metastable ligand in most surficial environments and has a high affinity to complex most divalent metals. This sulfide-complexing effect is particularly strong for mercury, which has a logarithmic mercuric-sulfide solubility product of approximately  $-50$  (Hogfeldt, 1983). At thermodynamic equilibrium, the product of the molar concentrations of uncomplexed mercury and uncomplexed sulfide ions is therefore expected to be very low (of the order of  $10^{-50}$ ) due to the formation of mercuric sulfide. As the presence of DOC facilitates the dissolution or desorption of particle-associated mercury, and subsequent flux of dissolved mercury species, the presence of sulfides can conversely facilitate precipitation and decreased solubility of mercury, inhibiting benthic flux.

5. **Dissolved organic carbon (DOC):** DOC concentrations serve as an indicator of the presence of organic ligands that can complex and enhance the solubility of trace metals including mercury (Kuwabara and others, 2003a). The partitioning and speciation of certain metals in aquatic systems are significantly affected by organic complexation (Mantoura and others, 1978; McKnight and others, 1983), and this effect is particularly important for mercury. Ligands represented by dissolved organic carbon can compete with sulfide to regulate mercury solubility and hence mobility (see section 7 below, Ravichandran and others, 1998) and can also decrease the bioavailability of mercury to certain aquatic biota (Sjoblom and others, 2000).

The benthic flux of DOC was dramatically different between seasons with November values much higher than those in May ([Table 6; Fig. 5](#)). This difference was most dramatic at Station 29A where May values averaged 27 micromoles per square meter per hour, while in November this value averaged 1302. At Station 25, these values were -135 and 371, respectively. Despite this dramatic change in values, and the afore-mentioned potential DOC regulation of mercury solubility, the mercury flux values were relatively consistent ([mercury discussion](#)). Negative DOC fluxes (that is DOC consumed by the sediment), as observed at Station 25 in May, have been reported, but are atypical (Caffrey and others, 1996). However, individual cores, but not site averages, showed negative DOC fluxes in Topping and others, 2001.

DOC bottom-water concentrations varied little temporally at Station 25. At Station 29A, while they did not exhibit a water-column concentration gradient in either season, the bottom-water concentration was much lower in November (154 micromolar) than May (219 micromolar). If sediment porewater concentrations remained the same, the low November value would have created a larger concentration gradient, and this could account for the increased DOC flux at Station 29A in November. Although the relationship was not linear, the highest bottom-water DOC concentration corresponded to the highest dissolved total mercury concentration (Station 25 in May).

6. **Benthic flux of other dissolved metals:** Additional dissolved metals, nickel and copper, were analyzed and compared to previous measurements to determine how 2003 compares in terms of metal mobilization. Dissolved-metal concentrations for nickel (Ni) in the water column did not indicate a vertical concentration gradient ([Table 8](#)). For nickel, concentrations in the bottom water were generally lower in 2003 than 1998/1999 (Topping and others, 2001). At Station 25, this was most pronounced in the fall (23 nanomolar in 2003, 43 in 1998/99) but was also witnessed in the spring

samplings (30; 34). Station 29A, with only a spring comparison possible, reflected this trend as well (25; 28).

Copper (Cu) concentrations ([Table 8](#)) weren't previously published in Topping and others, 2001, so no semi-decadal comparisons can be made. However, copper concentrations were significantly lower in the bottom water relative to the surface and mid-depth at Station 29A in May 2003. This is indicative of either a benthic sink or a water-column source. This vertical gradient was not observed in November 2003.

Dissolved-nickel benthic flux in 2003 was anomalous relative to values from the previous five years using the same methods at the same stations (Topping and Kuwabara, 2003). From 1998 through spring 2002, only 4 individual cores out of 34 exhibited a negative flux. In 2003, 5 of 12 values were below zero, with all five occurring from Station 25 samples. In fact, the average for all Station 25 flux estimates in 2003 was  $-10 \pm 22$  (n=6) nanomoles per square meter per hour, while at Station 29A this value was  $62 \pm 47$  (n=6). This higher nickel flux at Station 29A relative to Station 25 was also observed from 1998 through spring 2002, but to a lesser extent.

Dissolved-copper benthic flux was also somewhat unusual in 2003. Although copper fluxes were variable in direction, the majority were negative, and the mean of all 2003 values ( $-35 \pm 37$  nanomoles per square meter per hour, n=12) is appreciably lower than those observed in Topping and others, 2001 (approximately 3 nanomoles per square meter per hour).

Combined, these data suggest that conditions during our sampling events in 2003 were less conducive to metal remobilization and release from bed sediments than previously observed. This indicates that estimates of long-term mercury flux could be incorrectly low if based only on 2003 sampling. However, others have found little relationship between mercury flux and the flux of other trace metals (R. Mason – personal communication, Sept. 2004).

**7. Nutrient benthic flux:** Dissolved nutrients exhibited interesting trends with regards to benthic flux.

Ammonia flux was noticeably higher in May relative to November ([Table 9](#)), and this temporal shift was most prominent at Station 25. Higher ammonia flux is often associated with more reducing conditions; however, this is not consistent with ancillary sediment characterization data ([Table 10](#)) which showed both stations to be more reducing in November.

Orthophosphate fluxes, which are often linked to adsorption-desorption reactions onto ferric oxide surfaces, showed no significant temporal change, but did show a prominent spatial difference. Fluxes were all below zero at Station 29A, but all positive at Station 25. The negative values at Station 29A are not necessarily indicative of regular conditions: Topping and others, 2001, found positive orthophosphate fluxes at Station 29A in May 1999 (no nutrient flux data was available for Station 25).

In aquatic systems where phytoplankton assemblages are dominated by diatoms, benthic fluxes of silica are used to estimate the dissolution of biogenic bed material. The conventional assumption is that diatom frustules are the major silica source to the surficial bed sediment. Our data appears to corroborate this since silica fluxes were higher for May samples, which were taken following the spring phytoplankton bloom. The subsequent gravitational settling and degradation of these siliceous frustules leads to an increased silica flux.

## Ancillary Sediment Characterization

The following data, which were not part of the original study, are included for two reasons: 1) To increase our understanding of the sediment at these sites and dates, and 2) To exhibit the suite of parameters that can be studied at a given site.

**Sediment Dynamics:** Using a technique which compares historical bathymetry data, Foxgrover and others (2004) have concluded that both stations in this study are likely to be sites of relatively recent deposition. Station 25 was apparently depositional from 1956 until 1983, the date of the last complete bathymetric survey, while station 29A appeared to be depositional from 1898 through 1983. Thus, all the current sediment is presumed to be relatively new. However, this new sediment is of unknown origin. In other words, it could be from the riverine inputs, or it could be from hydrodynamic resuspension in other regions of the estuary (potentially nearby areas which are considered likely to erode).

**Sediment Chemistry:** Since the focus of this project was benthic-flux measurements and overlying water characterization, this report does not provide a detailed explanation of all ancillary sediment results. However, [Table 10](#) provides general characterization of the temporal and spatial sediment conditions for a number of relevant parameters (e.g. sulfur and iron speciation data).

As noted in the [methods](#) section, the spring 2003 sediment was collected eight days earlier than the whole cores and overlying water collected for mercury flux measurements and water-column data. The site locations were identical, however, and the comparisons should be relevant given the seasonal comparison.

- Loss on ignition analysis (loss of organic matter upon application of heat) showed a higher amount of organic matter was present in the spring sediment than the autumn sediment at both stations ([Table 10](#)).
- Sediment Eh (a measurement of reducing/oxidizing conditions) showed that sediment at both stations was more reducing in the autumn than in the spring, and that Station 29A was more reducing than Station 25 in both seasons ([Table 10](#)). However, all values were positive, indicating oxidizing conditions.

Below, four relationships between aqueous and sediment data are discussed in detail.

1. **Sediment mercury concentration vs. Mercury flux:** The consistently positive dissolved mercury flux ([Table 4](#)) exhibited a strong positive correlation ( $r^2=0.69$ ; [Fig. 8](#)) to the concentration of mercury in the sediment ([Table 10](#)). Through dissolution and sorption reactions, accumulated mercury is partitioned between the bed sediment and interstitial waters. The dissolved-concentration gradient between the porewater and the overlying water drives a benthic flux of dissolved mercury out of or into the sediment. Acknowledging that only six flux measurements for dissolved mercury are involved in this one-year study, this correlation provides direct, supporting evidence for increased benthic flux of dissolved mercury due to elevated concentrations of mercury in the sediment.

2. **Net methylation potential vs. Sulfide flux:** Sulfide flux ([Table 5](#)) showed a strong positive correlation ( $r^2=0.72$ ; [Fig. 8](#)) to the ratio of the potentials for methylation and demethylation of mercury by microbes ([Table 10](#)). Methylation and sulfate reduction both occur as a result of transformations by taxonomically related bacteria in the sediment and under anoxic conditions. Sulfate reduction would increase sulfide

concentrations, and the resulting stronger concentration gradient would propagate the flux of sulfides into the water-column.

3. **Porewater sulfide vs. Mercury flux:** Although only one measurement for porewater sulfide ([Table 10](#)) was above detection limits (Station 29A, April), this corresponded to the site/date with the highest dissolved mercury flux value ([Table 4](#)). This correlation represents the high binding affinity between mercury and sulfide. Even with limited data, such significant correlations can be used as a screening tool to guide future management and research efforts.

4. **Porewater DOC vs. DOC flux:** The strong positive correlation ( $r^2=0.94$ ; [Fig. 8](#)) between dissolved organic carbon (DOC) concentrations in the porewater ([Table 10](#)) and DOC fluxes ([Table 6](#)) illustrates how concentration gradients drive benthic flux.

## Study Design and Methods

The protocol described in this section focuses on method applications in this series of two core-incubation experiments. Details (for example, quality control specifications) for each analysis have been previously documented (Woods and others, 1999; Praskins and others, 2001; Kuwabara and others, 2003a).

Sampling was performed at two U.S. Geological Survey (USGS) designated stations ([Fig. 1](#)) in the South Bay: numbers 25 (a western shoal station with fine silt/clay-textured bottom sediment) and 29A (a main channel station with sediment texture similar to Station 25). The stations are located 10.3 and 1.4 km south of the San Mateo Bridge, respectively (all stations are north of the Dumbarton Bridge). Samples were collected near slack tide before ebb. Therefore, the depths of the shoal station (25) was <2 m, and the main-channel station (29A) depth varied between 13 and 14 m.

### Coring Operation

On both sampling days (May 6 and November 12, 2003), three cores were collected at each of the two sites using a 28-kilogram coring device fabricated from non-metallic parts ([Fig. 3](#)) produced by Savillex Corporation, Minnetonka, Minnesota. To avoid sample contamination, wetted surfaces of the coring device and core tubes were acid-washed polypropylene or fluoroethylene polymer. Cores were collected in 10-centimeter diameter fluoroethylene polymer tubes 28-centimeters long. A tube, mounted on the coring device, was dropped onto the sediment by gravity, impacting the surface at about 0.2 meters per second and penetrating about 10 centimeters (depending on the porosity). Excessive penetration by the core was mitigated by four radially positioned, cylindrical weights that acted as stabilizers (or feet) for the device. This sampling protocol was designed to provide minimal disturbance or compression of soft sediments as visually verified by: (1) the presence of oxic sediment, (2) the presence of macroinvertebrates and their tubes, and (3) minimal resuspension of surficial sediment in the overlying water when the core was retrieved. If the sampler captured at least 2 centimeters of compacted silt or clay below the surficial layer, the sampler generally could be retrieved with the core and overlying water intact. Some samples were lost during retrieval, probably because the lowest sampled material was sandy or otherwise unconsolidated.

Immediately after retrieval, the bottom and top of the sample tube were capped with an insert on the bottom and a screw cap on the top (both made of fluoroethylene polymer). The tubes were stored upright in a padded plastic bin. To maintain ambient temperature, the bins were partially filled with bay water and covered with opaque plastic sheeting.

### Core Incubations

After cores were collected, samples were taken to nearby Menlo Park, California for processing in a constant-temperature room set to the ambient temperature. Cores were left overnight to equilibrate with wetted surfaces. Core incubations ([Fig. 7](#)) then began with the replacement of overlying water with bottom water that had been pumped from each site. Disturbance of the cores during handling was monitored by comparison of the chemical composition of the overlying water at the beginning of the incubation with bottom waters. Significant deviations in the composition of these water samples would indicate substantial disturbance of the core during processing.

Bottom water was aerobic on both sampling dates at both sites. The twelve cores taken at those sites were aerated overnight to condition wetted surfaces before the incubation period (Topping and others, 2001). Three of the four cores per site were selected for incubation on the basis of visual inspection of the sediment-water interface for any disturbances. Water overlying the sediment in the selected cores was sampled at four time intervals during a 12-hour incubation at the bottom-water temperature. Overlying water sampled from the cores was replaced by pumped bottom water from the site where the core was collected. A linear regression of the time series of solute concentrations was used to determine the benthic flux (slope of the time series) from each of the incubated cores. This regression generates a correlation ( $r^2$ ) of the solute concentration versus time.

When used to discuss data, the term “significant” is used in the text to indicate that two values were separated by more than their error (standard deviation or confidence interval).

## Physical Data

**Sediment Porosity:** After core incubations, approximately 10 milliliters of surficial sediment was collected from each core (top 3 centimeters) using a modified 10-cubic centimeter syringe. Wet weight and dry weight after lyophilization were measured to calculate porosity.

## Biological Data

1. **Benthic Macroinvertebrates:** After core incubations, each core was sieved (500-micrometer mesh). The sieved samples were fixed with 10-percent buffered formalin, later transferred to 70-percent ethanol, then sorted at 10× magnification and identified to the lowest practicable taxonomic level employing the appropriate literature ([Fig. 10](#)). Samples were stained with rose bengal to facilitate sorting. No subsampling was used.
2. **Benthic Chlorophyll-*a*:** Each incubated core was sub-sampled in triplicate for benthic chlorophyll-*a*. Surficial sediment (top 0.5 centimeters) was collected on a glass-fiber filter and buffered with magnesium carbonate. Samples were then frozen in darkness for preservation until spectrophotometrically analyzed by methods described in Thompson and others (1981) and Franson (1985) ([Fig. 11](#)).

## Chemical Parameters

1. **Bottom-water sampling:** Prior to coring at each sampling site, bottom-water samples (approximately 1 meter above the sediment-water interface) were collected for subsequent analysis of dissolved-mercury speciation by cold-vapor atomic fluorescence spectroscopy (CVAFS) using a high-displacement peristaltic pump and a tethered length of rigid fluoroethylene polymer tubing. These samples were also used to replace overlying water in cores collected from each site for incubation.
2. **Dissolved Oxygen (DO):** Concentrations of dissolved oxygen were monitored for each incubated core using a micro-Winkler titration method ([Fig. 12](#); Kuwabara and others, 2000).
3. **Dissolved Mercury and Methyl Mercury:** Dissolved-mercury and methyl-mercury samples were processed in a Class-100 laminar-flow hood. Samples from water-column sampling, and core incubations were filtered with 0.7-micrometer quartz membranes that had been baked for 6 hours at 500 degrees centigrade to remove residual organics. Filtered samples were acidified with quartz-distilled nitric acid (pH less than 2), and refrigerated in darkness until analyzed by CVAFS ([Fig. 13](#), Krabbenhoft and others, 1998). Methodological details were reported by DeWild and others (2002).
4. **Dissolved Trace Metals by ICP-MS:** Water-column samples were also collected, filtered (0.2-micrometer polycarbonate membrane) and acidified to provide dissolved trace-metal information for the estuary by flow-injection inductively coupled plasma mass spectrometry (Topping and Kuwabara, 1999; [Fig. 14](#)).
5. **Dissolved nutrients:** Nutrient samples were filtered (0.2-micron polycarbonate membranes) and immediately refrigerated in darkness. Unlike trace-metal samples, nutrient samples were not acidified. Concentrations for dissolved (0.2-micron filtered) nitrate, ammonia, orthophosphate and silica were determined by automated spectrophotometry ([Fig. 15](#)).
6. **Dissolved organic carbon (DOC):** Dissolved organic carbon was determined by high-temperature, non-catalytic combustion (Qian and Mopper, 1997). Potassium phthalate was used as the standard.

Low-DOC water (blanks <40 micrograms-organic carbon per liter) was generated from a double-deionization unit with additional ultraviolet treatment (Milli-Q Gradient, Millipore Corporation) ([Fig. 16](#)).

7. **Dissolved Sulfides:** Dissolved sulfides in overlying-water samples were analyzed by square-wave voltammetry ([Fig. 17](#); Kuwabara and Luther, 1993).

### Ancillary Sediment Characterization

1. **Sediment sampling:** Sediment was taken from both sites on April 28th 2003 and November 12th 2003 to generate ancillary data ([Table 10](#)) for comparisons to the benthic flux and water-column data. For both samplings, the surface 0-4 cm depth interval of sediment was collected and transferred into glass mason jars, which were filled to the top to exclude oxygen and stored on ice during transit and later refrigerated (5 °C) until sub-sampling the following day. All sampling equipment was acid cleaned prior to use. All initial sediment processing for microbial assays and ancillary sediment characterization was conducted in a nitrogen gas (N<sub>2</sub>) flushed glove bag to maintain anaerobic conditions. Sediment from a single site was transferred to a clean zip-lock bag and manually homogenized. Sub-samples, for each process or analyte, were taken from this composite sample. Sediment pore water was collected via centrifugation under anoxic conditions.
2. **Microbial Rate Assays:** The addition of radio-labeled inorganic mercury (<sup>203</sup>Hg(II)) and methylmercury (<sup>14</sup>CH<sub>3</sub>MeHg<sup>+</sup>) to whole sediment was used to measure potential rates of methyl mercury production and degradation, respectively (Marvin-DiPasquale and others, 2003; Marvin-DiPasquale and Oremland 1998). Microbial sulfate reduction was similarly assayed in whole sediment using the radioactive sulfate (<sup>35</sup>SO<sub>4</sub><sup>2-</sup>) amendment method (Jørgensen 1978). All samples were incubated for four hours at in situ temperatures (April 2003 = 15 °C, November 2003 = 21 °C).
3. **Sediment Mercury Speciation:** Sediment total mercury was assayed by nitric/sulfuric acid digestion, bromine chloride (BrCl) oxidation to Hg(II), tin chloride (SnCl<sub>2</sub>) reduction to gaseous Hg<sup>0</sup>, purge and trapping of Hg<sup>0</sup> on gold coated glass beads, and finally Hg<sup>0</sup> quantification via cold vapor atomic fluorescence spectroscopy (Gill and Fitzgerald 1987, Bloom and Fitzgerald, 1988).  
Reactive Hg(II) was assayed as per total mercury, except without pre-digestion of the sample with nitric/sulfuric acid, followed by BrCl oxidation. SnCl<sub>2</sub> was added to a 0.3 g sediment sample diluted in 50 ml trace clean anoxic water. The amount of Hg(II) chemically reduced to Hg<sup>0</sup> and captured on the gold trap after 30 minutes of purging with helium, was operationally defined as the “reactive” Hg(II) fraction.
4. **Sediment Organic Content:** Measured by weight loss on ignition to 500 °C for 4 hours (APHA, 1981).
5. **Sediment Acid Volatile Reduced Sulfur:** Measured by the addition of 6 molar hydrochloric acid (6M HCl) to whole sediment, with the subsequent trapping of liberated gaseous sulfide in 10% zinc acetate solution. Sulfide was then assayed colorimetrically (Cline 1969). This primarily represents the solid phase iron sulfide (FeS) mineral fraction.
6. **Sediment Total Reduced Sulfur:** Measured by the addition of 6 molar HCl and 1 molar chromium (II) (1 M Cr(II)) to whole sediment, with the subsequent heated distillation and trapping of liberated gaseous sulfide in 10% zinc acetate solution. Sulfide was then assayed spectrophotometrically (Cline 1969). This primarily represents the combined solid phase FeS and pyrite (FeS<sub>2</sub>) mineral fractions, as well as elemental sulfur (S<sup>0</sup>).

7. **Sediment Ferrous Iron:** Measured by extraction of iron (II) (Fe(II)) using 0.5 molar HCl followed by quantification with ferrozine (Lovley and Phillips, 1987).
8. **Sediment Amorphous Ferric Iron:** Measured by extraction of Fe(II) using 0.5 molar HCl followed by reduction of Fe(III) to Fe(II) with hydroxylamine, and quantification with ferrozine (Lovley and Phillips, 1987). This is the fraction of Fe(III) that is most available to iron-reducing bacteria.
9. **Sediment Crystalline Ferric Iron:** Measured by the reductive dissolution of Fe(III)-oxide mineral phases with citrate-dithionite extraction, followed quantification with ferrozine (Roden and Zachara, 1996).
10. **Sediment pH and Redox:** Both parameters measured both via electrode inserted directly into sediment.
11. **Pore-water Ferrous Iron:** Measured spectrophotometrically with ferrozine (USEPA, 1996). This provides an indication of microbial Fe(III)-reduction activity.
12. **Pore-water Sulfate and Chloride:** Assayed via ion chromatography (Dionex, 1992).
13. **Pore-water Dissolved Organic Carbon (DOC):** Measured via high temperature oxidation with IR detection (Qian and Mopper, 1996).
14. **Pore-water Sulfide:** Samples preserved with sulfide anti-oxidizing buffer and assayed via ion specific electrode (Gilmour, 1998).

## References Cited

- Abu-Saba, K.E., and Tang, L.W., 2000, Watershed Management of Mercury in the San Francisco Bay Estuary: a TMDL Report to the U.S. EPA (Internet access at: <http://www.swrcb.ca.gov/rwqcb2/download/aug00HgTMDL.pdf>)
- Aller, R.C., and Aller, J.Y., 1998, The effect of biogenic irrigation intensity and solute exchange on diagenetic reaction rates in marine sediments: *Journal of Marine Research*, v. 56, p. 905-936
- Alpers, C.N., and Hunerlach, M.P., 2000, Mercury contamination from historic gold mining in California: U.S. Geological Survey Fact Sheet FS-061-00, 6 p. (Internet access at: <http://ca.water.usgs.gov/mercury/fs06100.html>).
- APHA, 1981, Section 209 G: Volatile and fixed matter in non-filterable residue and in solid and semisolid samples. In: Franson MAH (ed) *Standard Methods for the Examination of Water and Wastewater*, 15th Edition. American Public Health Association, American Water Works Association, Water Pollution Control Federation, Washington, D.C., p. 97-99
- Bloom, N.S., Fitzgerald, W.F., 1988, Determination of volatile mercury species at the picogram level by low-temperature gas chromatography with cold-vapor atomic fluorescence detection: *Analytica Chimica Acta.*, v. 208, p. 151-161
- Caffrey, J.M., Hammond, D.E., Kuwabara, J.S., Miller, L.G., and Twilley, R.R., 1996, Benthic processes in San Francisco Bay: the role of organic inputs and bioturbation, in Hollibaugh, J.T., ed., *San Francisco Bay: the Ecosystem: American Association for the Advancement of Science, Pacific Division, San Francisco*, p. 425-442.
- Charbonneau, P., Hare, L., and Carignan, R., 1997, Use of X-ray images and a contrasting agent to study the behavior of animals in soft sediments: *Limnology and Oceanography*, v. 42, p. 1823-1828.
- Cheng, R.T. and Gartner, J.W., 1985, Harmonic analysis of tides and tidal current in South San Francisco Bay, California: *Estuarine, Coastal and Shelf Science*, v. 21, p. 57-74.
- Choe, K.Y., Gill, G.A., Lehman, R.D., Han, S., Heim, W.A. and Coale, K.H., 2004, Sediment-water exchange of total mercury and monomethyl mercury in the San Francisco Bay-Delta: *Limnology and Oceanography*, v. 49, p. 1512-1527.
- Cline, J.D., 1969, Spectrophotometric determination of hydrogen sulfide in natural waters: *Limnology and Oceanography*, v. 14, p. 454-458.
- Cloern, J.E., 1996, Phytoplankton bloom dynamics in coastal ecosystems: A review with some general lessons from sustained investigation of San Francisco Bay, California: *Reviews of Geophysics*, v. 34, No. 2, p. 127-168.
- Cloern, J.E., Schraga, T.S., Lopez, C.B., and Labiosa, R., 2003, Lessons from monitoring water quality in San Francisco Bay: 2003 Pulse of the Estuary, San Francisco Estuary Institute, p. 15-20 (Internet access at: <http://www.sfei.org/rmp/pulse/pulse2003.pdf>)
- Conaway, C.H., Squire, S., Mason, R.P., Flegal, A.R., 2003, Mercury speciation in the San Francisco Bay estuary: *Marine Chemistry*, v. 80, p. 199-225
- DeWild, J.F., Olson, M.L., and Olund, S.D., 2002, Determination of Methyl Mercury by Aqueous Phase Ethylation, Followed by Gas Chromatographic Separation with Cold Vapor Atomic Fluorescence Detection: Open-File Report 01-445 (Internet access at: <http://wi.water.usgs.gov/pubs/ofr-01-445/ofr-01-445.pdf>).
- Dionex. 1992, Installation Instructions and Troubleshooting Guide for the IONPAC AG4A-SC Guard Column / IONPAC AS4A-SC Analytical Column. Dionex Corporation Document No. 034528, 1992.
- Fischer, H.B., List, E.J., Koh, R.C.Y., Imberger, J., and Brooks, N.H., 1979, *Mixing in Inland and Coastal Waters*: Academic Press, Inc., Orlando, Florida, 483, p.

- Flegal, A.R., Smith G.J., Gill, G.A., Sanudo-Wilhelmy, S.A., Scelfo, G.M., and Anderson, L.C.D., 1991, Dissolved trace element cycles in the San Francisco Bay estuary: *Marine Chemistry*, v. 36, p. 329–363.
- Foxgrover, A.C., Higgins, S.A., Ingraca, M.K., Jaffe, B.E., Smith, R.E., 2004, Deposition, Erosion, and Bathymetric Change in South San Francisco Bay: 1858-1983: U.S. Geological Survey Open-File Report 04-1192, 25 p. (Internet access at: <http://pubs.usgs.gov/of/2004/1192/>)
- Franson, M.A.H., 1985, Standard methods for the examination of water and wastewater, Sixteenth Edition, Method 1003C.6: American Public Health Association, American Water Works Association, Water Pollution Control Federation, Washington, D.C., 1268 p.
- Gill, G.A., Fitzgerald, W.F., 1987, Picomolar mercury measurements in seawater and other materials using stannous chloride reduction and two-stage gold amalgamation with gas phase detection: *Marine Chemistry* v. 20 p. 227-243
- Gilmour, C.C., Riedel, G.S., Ederington, M.C., Bell, J.T., Benoit, J.M., Gill, G.A., and Stordal, M.C., 1998, Methylmercury concentrations and production rates across a trophic gradient in the northern Everglades: *Biogeochemistry*, v. 40, no. 2-3, p. 327-345.
- Goodridge, J., 2000, California Weather CD; CD-ROM prepared with support from California Department of Water Resources, Mendocino, CA
- Goss, H.R., 1958, The Life and Death of a Quicksilver Mine: Historical Society of Southern California, Los Angeles, California, 150 p.
- Grenz, C., Cloern, J.E., Hager, S.W., and Cole, B.E., 2000, Dynamics of nutrient cycling and related benthic nutrient and oxygen fluxes during a spring phytoplankton bloom in South San Francisco Bay (USA): *Marine Ecology Progress Series*, v. 197, p. 67–80.
- Hogfeldt, E., 1983, Stability constants of metal-ion complexes. Part A, Inorganic ligands. Pergamon Press, Oxford. 310 p.
- Johnson, K.M., 1963, The New Almaden Quicksilver Mine: The Talisman Press, Georgetown, California, 115 p.
- Jørgensen, B.B., 1978, A comparison of methods for the quantification of bacterial sulfate reduction in coastal marine sediments. 1. Measurement with radiotracer techniques: *Geomicrobiology Journal*, v. 1, p.11-27.
- Krabbenhoft, D.P., Gilmour, C.C., Benoit, J.M., Babiarz, C.L., Andren, A.W., and Hurley, J.P., 1998, Methyl mercury dynamics in littoral sediments of a temperate seepage lake: *Canadian Journal of Fisheries and Aquatic Sciences*, v. 55, p. 835–844.
- Kuwabara, J.S., Chang, C.C.Y., and Pasilis, S.P., 1990, Effects of benthic flora on arsenic transport: *Journal of Environmental Engineering*, v. 116, p. 394–409.
- Kuwabara, J.S., and Luther, G.W., III, 1993, Dissolved sulfides in the oxic water column of San Francisco Bay, California: *Estuaries*, v. 16, p. 567–573.
- Kuwabara, J.S., Chang, C.C.Y., Khechfe, A.I., and Hunter, Y.R., 1996, Implications of dissolved sulfides and organic substances for the chemical speciation of trace contaminants in the water column of San Francisco Bay, California, in Hollibaugh, J.T., ed., *San Francisco Bay: the Ecosystem: American Association for the Advancement of Science, Pacific Division, San Francisco*, p. 157–172.
- Kuwabara, J.S., Topping, B.R. Coale, K.H., and Berelson, W.M., 1999a, Processes affecting the benthic flux of trace metals into the water column of San Francisco Bay, In Morganwalp, D.W., and Buxton, H.T., eds., U.S. Geological Survey Toxic Substances Hydrology Program--Proceedings of the Technical Meeting, Charleston, South Carolina, March 8–12, 1999--Volume 2--Contamination of Hydrologic Systems and Related Ecosystems: U.S. Geological Survey Water-Resources Investigations Report 99-4018B, p. 115–119 (Internet access at: [http://toxics.usgs.gov/pubs/wri99-4018/Volume2/sectionA/2214\\_Kuwabara/index.html](http://toxics.usgs.gov/pubs/wri99-4018/Volume2/sectionA/2214_Kuwabara/index.html)).

- Kuwabara, J.S., Berelson, W.M., Balistrieri, L.S., Woods, P.F., Topping, B.R., Steding, D. J., and Krabbenhoft, D.P., 2000, Benthic flux of metals and nutrients into the water column of lake Coeur d'Alene, Idaho: Report of an August, 1999 Pilot Study: USGS Water-Resources Investigations Report 00-4132, 74 p. (Internet access at: <http://water.usgs.gov/pubs/wri/wri004132/>).
- Kuwabara, J.S., Marvin-Dipasquale, M.C., Praskins, W., Byron, E., Topping, B.R., Carter, J.L., Fend, S.V., Parchaso, F., and Krabbenhoft, D.P., 2002, Flux of dissolved forms of mercury across the sediment-water interface in Lahontan Reservoir, Nevada: U.S. Geological Survey Water Resources Investigations Report 02-4138, 48 p. (Internet access at: <http://water.usgs.gov/pubs/wri/wri024138/>).
- Kuwabara, J.S., Alpers, C.N., Marvin-DiPasquale, M.C., Topping, B.R., Carter, J.L., Stewart, A.R., Fend, S.V., Parchaso, F., Moon, G.E. and Krabbenhoft, D.P., 2003a. Sediment-water Interactions Affecting Dissolved-mercury Distributions in Camp Far West Reservoir, California. U.S. Geological Survey Water Resources Investigations Report 03-0140 (Internet access at: <http://water.usgs.gov/pubs/wri/wri034140/>)
- Kuwabara, J.S., Woods, P.F., Berelson, W.M., Balistrieri, L.S., Carter, J.L., Topping, B.R., and Fend, S.V., 2003b, Importance of sediment-water interactions in Coeur d'Alene Lake, Idaho: Management Implications: Environmental Management, v. 32, p. 348-359.
- Lanyon, Milton and Bulmore, Laurence, 1967, Cinnabar Hills, The Quicksilver Days of New Almaden: Village Printers, Los Gatos, California, 128 p.
- Li, Y.H., and Gregory, S., 1974, Diffusion of ions in sea water and in deep-sea sediments: Geochimica et Cosmochimica Acta, v. 38, p. 703–714.
- Looker, R.E. And Johnson, B., 2003, Mercury in San Francisco Bay. Total Maximum Daily Load (TMDL) Project Report (Internet access at: <http://www.swrcb.ca.gov/rwqcb2/TMDL/SFBayMercury/SFBayMercuryTMDLProjectReport.pdf>)
- Lovley, D.R., Phillips, E.J.P., 1987, Rapid Assay for microbially reducible ferric iron in aquatic sediments: Applications of Environmental Microbiology, v. 53, p.1536-1540.
- Mantoura, R.F.C., Dixon, A., and Riley, J.P., 1978, The complexation of metals with humic materials in natural waters: Estuarine and Coastal Marine Sciences, v. 6, p. 387–408.
- Marvin-DiPasquale, M.C. and Oremland, R.S., 1998, Bacterial methylmercury degradation in Florida Everglades peat sediment. Environmental Science and Technology v. 32, p.2556-2563.
- Marvin-DiPasquale, M.C., Agee, J.L., Bouse, R.M., Jaffe, B.E., 2003, Microbial cycling of mercury in contaminated pelagic and wetland sediments of San Pablo Bay, California: Environmental Geology, v. 43, p.260-267.
- Mason, R.P. and Lawrence, A.L., 1999, Concentration, distribution, and bioavailability of mercury and methylmercury in sediments of Baltimore Harbor and Chesapeake Bay, Maryland, USA: Environmental Contamination and Toxicology, v. 18, p. 2438-2447.
- McKee, L., Leatherbarrow, J., Eads, R., and Freeman, L., 2004 (Draft), Concentrations and loads of PCBs, OC pesticides, and mercury associated with suspended sediments in the lower Guadalupe River, San Jose, California: A Technical Report of the Regional Watershed Program: SFEI Contribution #86. San Francisco Estuary Institute, Oakland, CA. ppxx
- McKnight, D.M., Feder, G.L., Thurman, E.M., Wershaw, R.L., and Westall, J.C., 1983, Complexation of copper by aquatic humic substances from different environments: Science of the Total Environment, v. 28, p. 65–76.
- Miller, D.C., 1984, Mechanical post-capture particle selection by suspension- and deposit-feeding *Corophium*: Journal of Experimental Biology and Ecology, v. 82, p. 59–76.
- Nichols, F.H., and Patamat, M.M., 1988. The Ecology of the Soft-Bottom Benthos of San Francisco Bay: A Community Profile. Biological Report 85 (7.19), September. Unites States Geological Survey and San Francisco State University

- Praskins, W., Byron, E., Marvin-DiPasquale, M.C., Kuwabara, J.S., Diamond, M.L., and Gustin, M.S., 2001, Sampling and Analysis Plan: Mercury Dynamics in Lahontan Reservoir: U.S. Environmental Protection Agency, March 22, 2001, 46 p.
- Qian, J.-G., and Mopper, K., 1996, Automated high-performance, high-temperature combustion total organic carbon analyzer: *Analytical Chemistry*, v. 68, p. 3090–3097.
- Ravichandran, M., Aiken, G.R., Reddy, M.M., and Ryan J.N., 1998, Enhanced dissolution of cinnabar (mercuric sulfide) by dissolved organic matter isolated from the Florida Everglades: *Environmental Science and Technology*, v. 32, p. 3305–3311.
- Rivera-Duarte, I. and Flegal, A.R., 1997, Pore-water silver concentration gradients and benthic fluxes from contaminated sediments of San Francisco Bay, California: *Marine Chemistry* v. 56 p.15-26
- Roden, E.E. and Zachara, J.M., 1996, Microbial reduction of crystalline iron (III) oxides: Influence of oxide surface area and potential for cell growth: *Environmental Science and Technology*, v. 30, p.1618-1628
- Rytuba, J.J., and Enderlin, D.A., 1999, Geology and environmental geochemistry of mercury and gold deposits in the northern part of the California coast range mercury mineral belt, In Wagner D.L., and Graham, S.A., eds., *Geologic Field Trips in Northern California, Centennial Meeting of the Cordilleran Section of the Geological Society of America: California Department of Conservation, Division of Mines and Geology, Special Publication 119*, p. 214-234.
- Schneider, Jimmie, 1992, *Quicksilver, the Complete History of Santa Clara County's New Almaden Mine*: Zella Schneider, San Jose, California, 178 p.
- Sjöblom, Å., Meili, M., and Sundbom, M., 2000, The influence of humic substances on the speciation and bioavailability of dissolved mercury and methyl-mercury, measured as uptake by *Chaoborus* larvae and loss by volatilization: *The Science of the Total Environment*, v. 261, p. 115–124.
- Tetra Tech, 2003. Technical Memorandum 2.2 Synoptic Survey Report. Guadalupe River Watershed Mercury TMDL Project. (Internet access at: [http://www.valleywater.org/media/pdf/Guad\\_River\\_TMDL/Guad\\_TMDL\\_Synoptic\\_Survey\\_Report.pdf](http://www.valleywater.org/media/pdf/Guad_River_TMDL/Guad_TMDL_Synoptic_Survey_Report.pdf))
- Thibodeaux, J.L., and Bierman, V.J., 2003, The bioturbation-driven chemical release process: *Environmental Science and Technology*, v. 37, no. 13, p. 251A–261A.
- Thomas, M.A., Conaway, C.H., Steding, D.J., Marvin-DiPasquale, M.C., Abu-Saba, K.E., and Flegal, A.R., 2002. Mercury contamination from historic mining in water and sediment, Guadalupe River and San Francisco Bay, California. *Geochemistry, Exploration, Environment, and Analysis*, 2, 211-217
- Thompson, J.K., Nichols, F.H., and Wienke, S.M., 1981, Distribution of benthic chlorophyll in San Francisco Bay, California, February 1980 – February 1981: U.S. Geological Survey Open File Report 81-1134, 55 p.
- Topping, B.R. and Kuwabara, J.S., 1999, Flow-injection-ICP-MS method applied to benthic-flux studies of San Francisco Bay, In Morganwalp, D.W., and Buxton, H.T., eds., U.S. Geological Survey Toxic Substances Hydrology Program--Proceedings of the Technical Meeting, Charleston, South Carolina, March 8–12, 1999--Volume 2--Contamination of Hydrologic Systems and Related Ecosystems: U.S. Geological Survey Water-Resources Investigations Report 99-4018B, p. 131-134 (Internet access at: [http://toxics.usgs.gov/pubs/wri99-4018/Volume2/sectionA/2216\\_Topping/index.html](http://toxics.usgs.gov/pubs/wri99-4018/Volume2/sectionA/2216_Topping/index.html)).
- Topping, B.R., Kuwabara, J.S., Parchaso, F., Hager, S.W., Arnsberg, A.J., and Murphy, F., 2001, Benthic flux of dissolved nickel into the water column of South San Francisco Bay: U.S. Geological Survey Open-file Report 01-89, 50 p. (Internet access at: <http://pubs.water.usgs.gov/ofr01089/>).
- Topping, B.R. and Kuwabara, J.S., 2003, Dissolved nickel and benthic flux in South San Francisco Bay: A potential for natural sources to dominate: *Bulletin of Environmental Contamination and Toxicology*, v. 71, p. 46-51.
- U.S. EPA, 1996, *Compilation of EPA's Sampling and Analysis Methods, Second Edition*: New York, CRC Press Inc., 1696 p.

- U.S. EPA. 1997. Mercury Study Report to Congress (Volumes I - IV). Washington D.C. (Internet access at: <http://www.epa.gov/oar/mercury.html>)
- Watras, C.J., Back, R.C., Halvorsen, S., Hudson, R.J.M., Morrison, K.A., and Wente, S.P., 1998, Bioaccumulation of mercury in pelagic freshwater food webs: *The Science of the Total Environment*, v. 219, p. 183-208.
- Wood, T.M., Baptista, A.M., Kuwabara, J.S., and Flegal, A.R., 1995, Diagnostic modeling of trace metal partitioning in south San Francisco Bay: *Limnology and Oceanography*, v. 40, p. 345-358.
- Woods, P.F., Nearman, M.J., and Barton, G.J., 1999, Quality assurance project plan for U.S. Geological Survey studies in support of Spokane River Basin RI/FS.: U.S. Environmental Protection Agency, Seattle, Washington, and U.S. Geological Survey, Boise, Idaho, 153 p.
- Word, J.Q., 1980, Classification of benthic invertebrates into infaunal trophic index feeding groups, Bascom, W., ed., *Biennial Report: Southern California Coastal Research Project*, Long Beach, CA, p. 103-121.

## **Acknowledgments**

The authors thank M. Olson, J. DeWild, and S. Olund (USGS, Madison, WI) for mercury-speciation analyses and J. Carter (USGS, Menlo Park, CA) for discussions regarding macroinvertebrates. The San Francisco Estuary Institute (SFEI Project Number RMP-440 / USGS Agreement 03H44559WFO003) and the USGS Toxic Substances Hydrology Program are gratefully acknowledged for support of this work, as is T. Mulvey for tireless efforts in support of water quality in San Francisco Bay. Helpful and thorough reviews by A. Foster and M. Hornberger (USGS, Menlo Park, CA) were appreciated.

Product names are provided for identification purposes only and do not constitute endorsement by the U.S. Geological Survey.

## Appendix 1: Comments on the Report Structure

A major objective of this electronic document is to provide a structure that is easily accessible to a wide range of interest groups. Therefore, pathways within this document have been constructed to be both logical and intuitive. In contrast to typical scientific manuscripts, this report is formatted in a pyramid-like structure to serve the needs of diverse groups who may be interested in reviewing or acquiring information at various levels of technical detail. The report enables quick transitions between the initial [summary information](#) (figuratively at the top of the pyramid) and the later details of [methods](#) or [results](#) (figuratively towards the base of the pyramid) using hyperlinks to supporting figures and tables, and an electronically linked [Table of Contents](#). In addition to hyperlinks within the document to supporting figures and tables, links in Appendices 2 and 3 provide a quick way to directly review and examine all figures and tables.

Although hard copies of this report are available on request, the advantages of the electronic version relative to the hard copy are substantial in many respects, but particularly in the rapid access of information at multiple levels of detail.

Your comments about how this type of Web-based product may be improved to better serve readers are most welcome and may be directed to the major author ([btopping@usgs.gov](mailto:btopping@usgs.gov)) so that they may be compiled for future revisions and reports.

## Appendix 2: List of Figures

- [Fig. 1](#) – Site map of the study area
- [Fig. 2](#) – Photos of historic mercury mining areas
- [Fig. 3](#) – Photos of the coring operation
- [Fig. 4](#) – Comparison of fluxes and riverine inputs of dissolved mercury
- [Fig. 5](#) – Strong seasonal changes in the benthic flux of DOC
- [Fig. 6](#) – Conceptual model of solute transport through a reservoir
- [Fig. 7](#) – Processes regulating benthic flux of solutes
- [Fig. 8](#) – Correlations between aqueous and sediment data
- [Fig. 9](#) – Incubation core design
- [Fig. 10](#) – Photo of macroinvertebrate taxonomy methods
- [Fig. 11](#) – Photo of benthic chlorophyll analyses
- [Fig. 12](#) – Photo of dissolved oxygen analyses
- [Fig. 13](#) – Photo of dissolved mercury analyses
- [Fig. 14](#) – Photo of dissolved metal analyses
- [Fig. 15](#) – Photo of dissolved nutrient analyses
- [Fig. 16](#) – Photo of dissolved organic carbon (DOC) analyses
- [Fig. 17](#) – Photo of dissolved sulfide analyses

### Appendix 3: List of Tables

<a href="#">Table 1</a>	– Benthic-invertebrate taxonomy
<a href="#">Table 2</a>	– Benthic-chlorophyll analyses
<a href="#">Table 3</a>	– Water-column concentrations for mercury species
<a href="#">Table 4</a>	– Dissolved mercury benthic fluxes
<a href="#">Table 5</a>	– Dissolved sulfide benthic fluxes
<a href="#">Table 6</a>	– Dissolved organic carbon (DOC) benthic fluxes and water-column concentrations
<a href="#">Table 7</a>	– Dissolved oxygen consumption
<a href="#">Table 8</a>	– Dissolved nutrient benthic fluxes
<a href="#">Table 9</a>	– Dissolved-copper and nickel benthic fluxes and water-column concentrations
<a href="#">Table 10</a>	– Ancillary sediment characterization

Figure 1. Benthic-flux Coring Sites

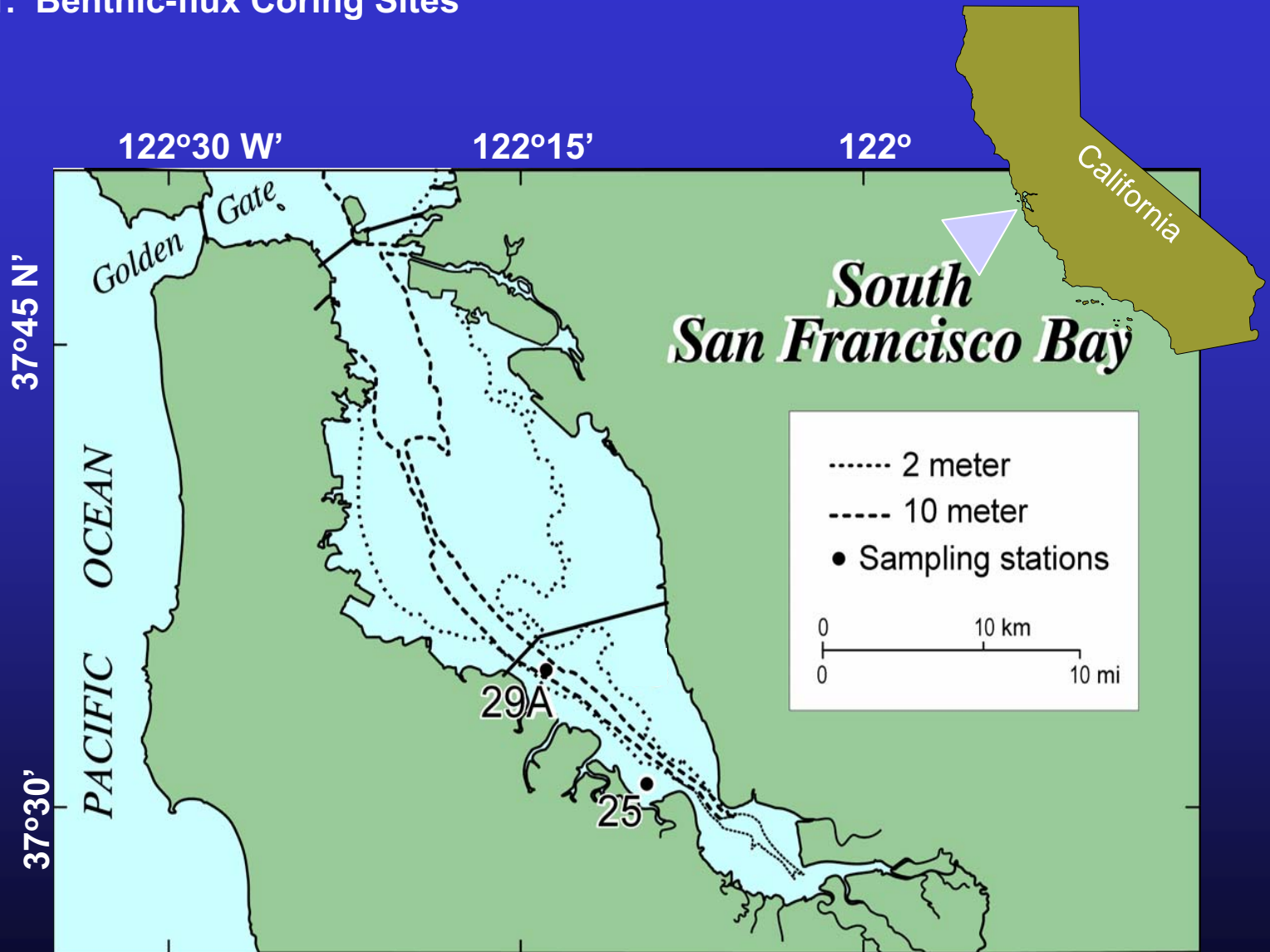


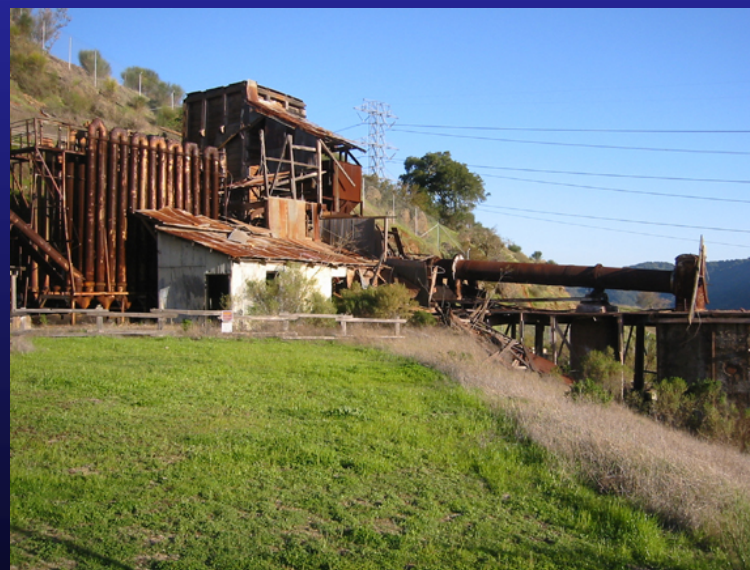
## Figure 2. Photos of Historic Mercury Mining Areas, Almaden-Quicksilver County Park, CA



Entrance to San Cristobal Tunnel; opened in 1866



Cinnabar ore within the mine



Rotary Furnace installed near Mine Hill in 1940 to increase output of mercury flasks to market

## Figure 3. Coring Operation



Coring apparatus with newly acquired core



Core kept for incubation

# Figure 4. Comparison of Benthic Flux to Riverine Inputs for Dissolved Mercury

Dissolved riverine loads estimated from Tetra Tech (2003); Particulate loads from Looker and Johnson (2003); Symbols represent individual core flux estimates, with station number enclosed and color/shape representing season (green/circle: spring; orange/triangle: fall)

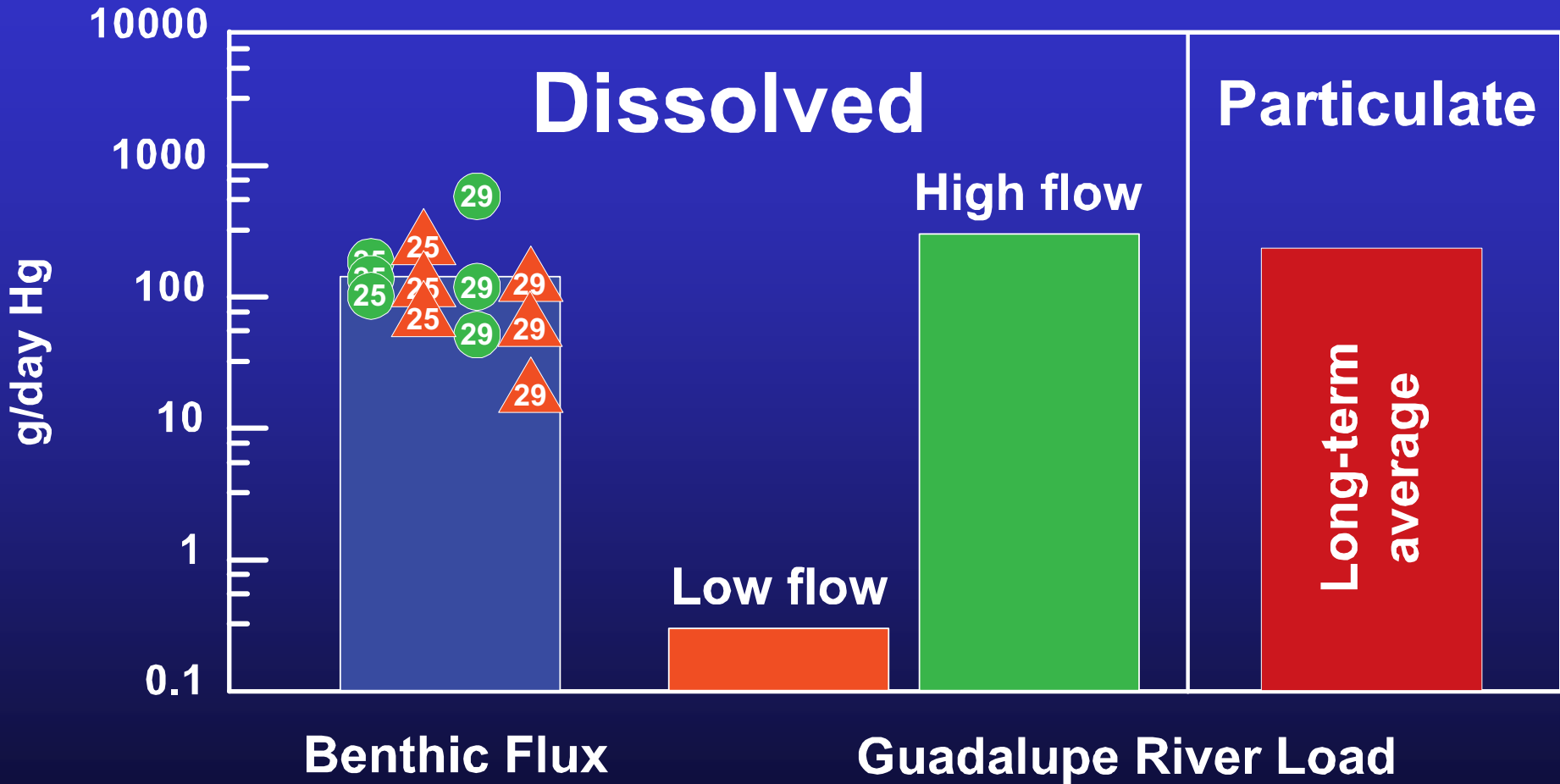


# Figure 5. Strong Seasonal Changes in the Benthic Flux of DOC

Error bars represent standard deviations of individual flux cores

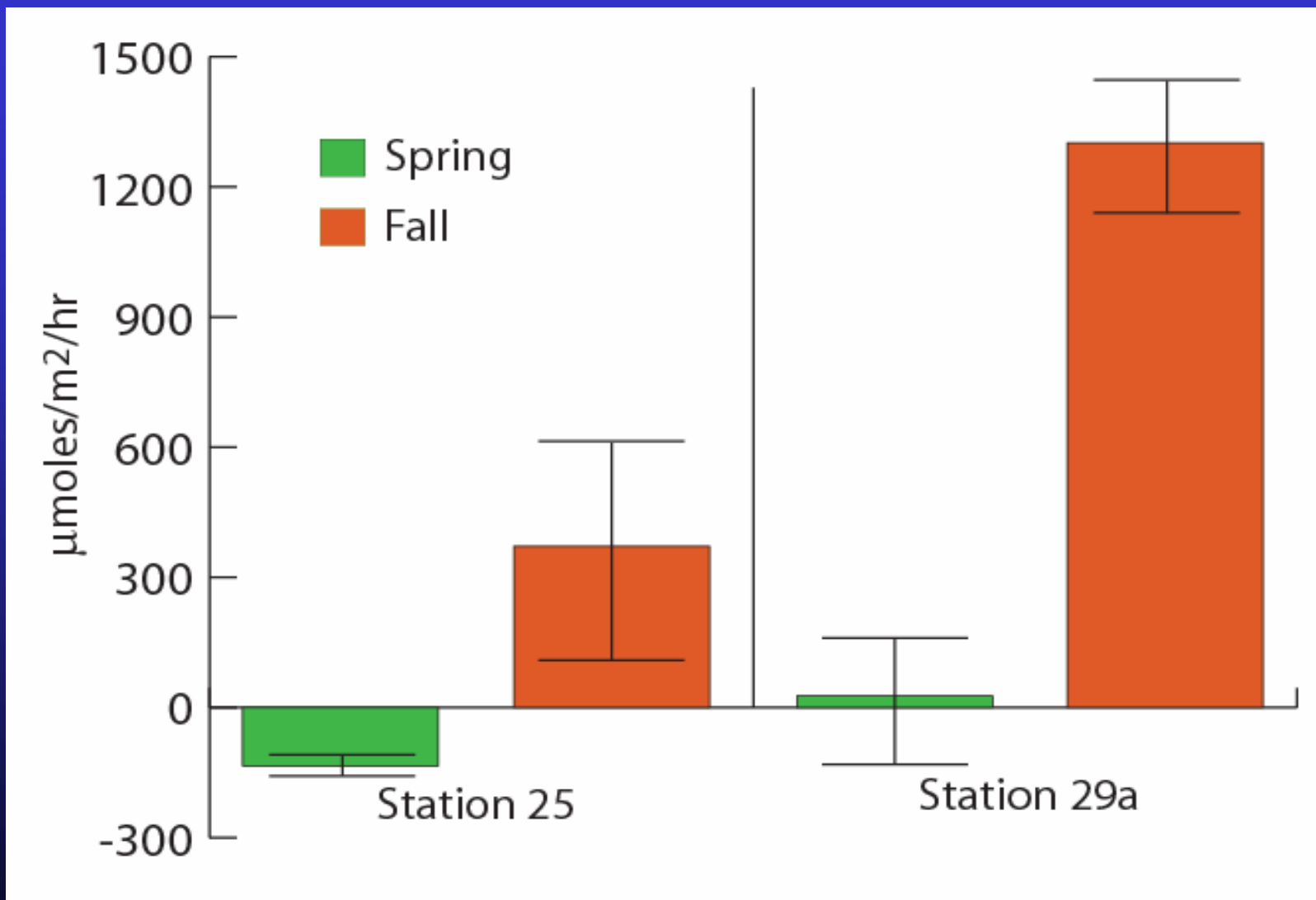


Figure 6.

# Processes Regulating Benthic Flux

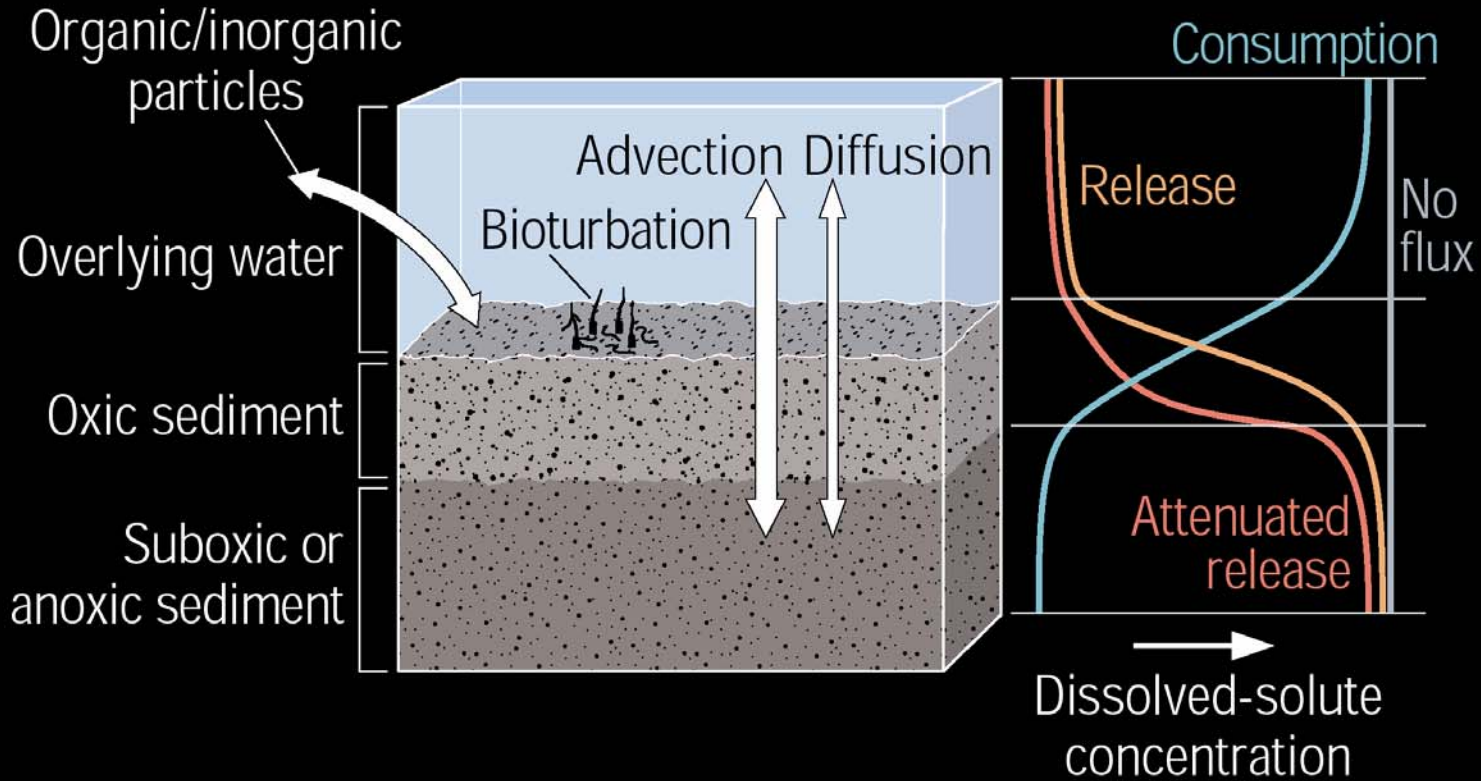
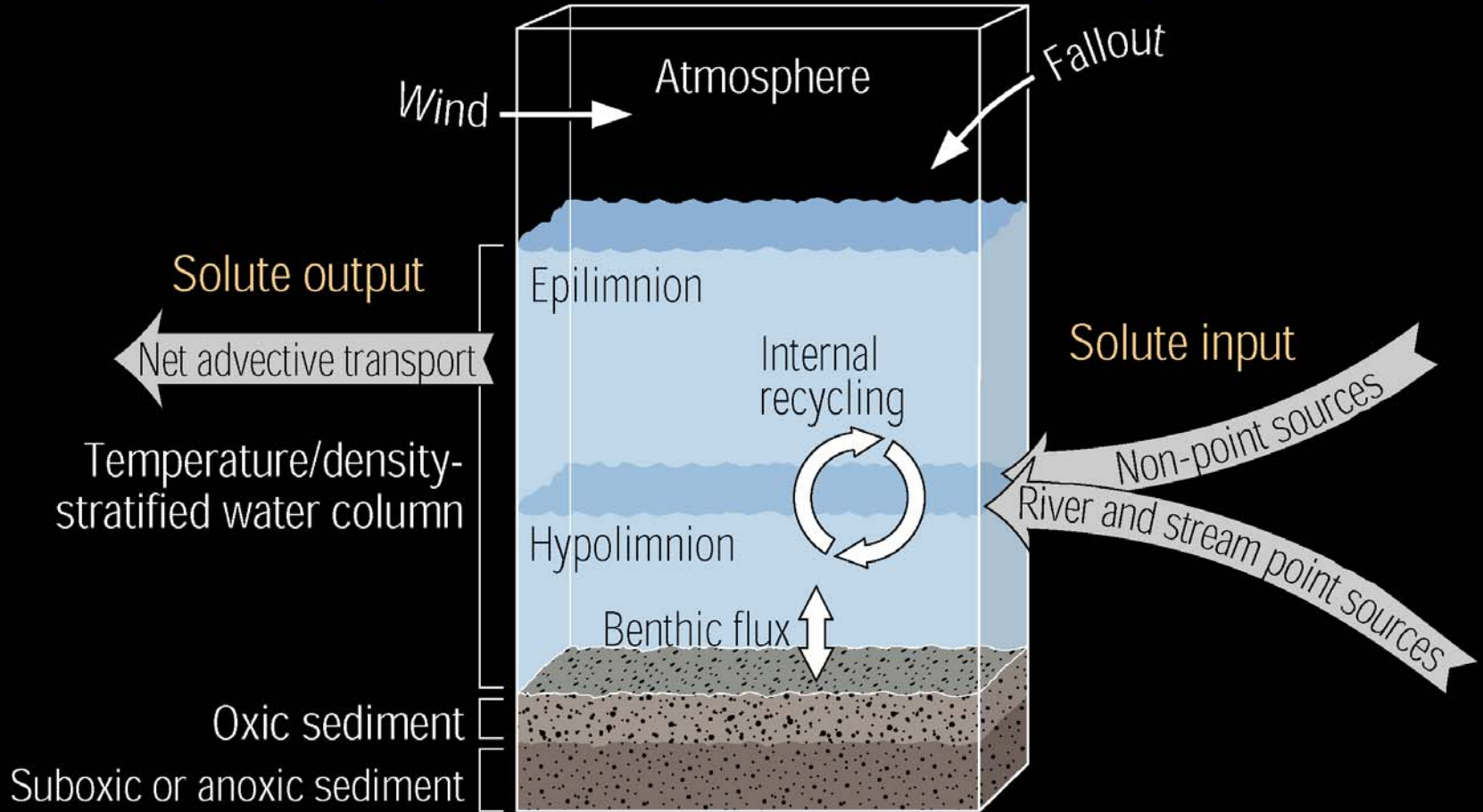


Figure 7.

# Conceptual Model of Solute Transport



## Figure 8. Correlations between Aqueous and Sediment Data

Including approximate linear fit and correlation coefficient;  
sediment data is plotted on the x-axis; aqueous data, y-axis;  
see [Ancillary Sediment Characterization](#)

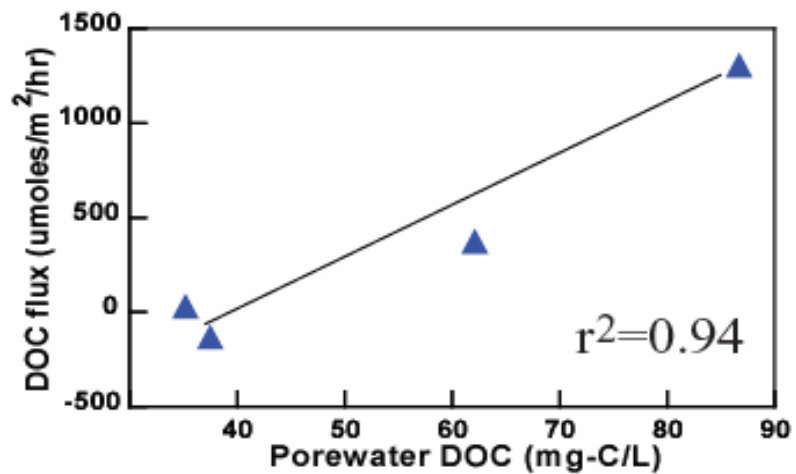
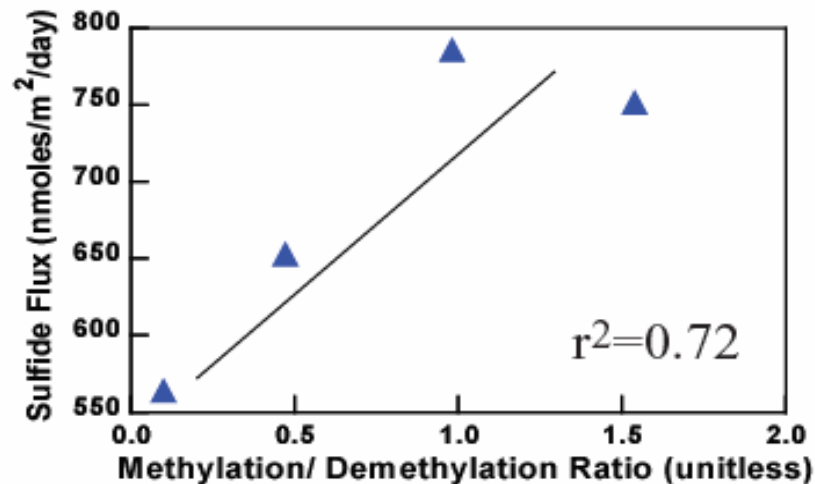
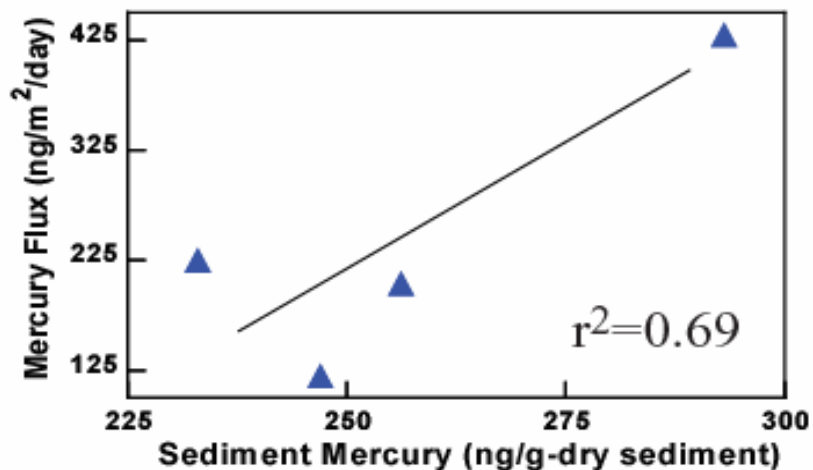


Figure 9. Incubation Core Design

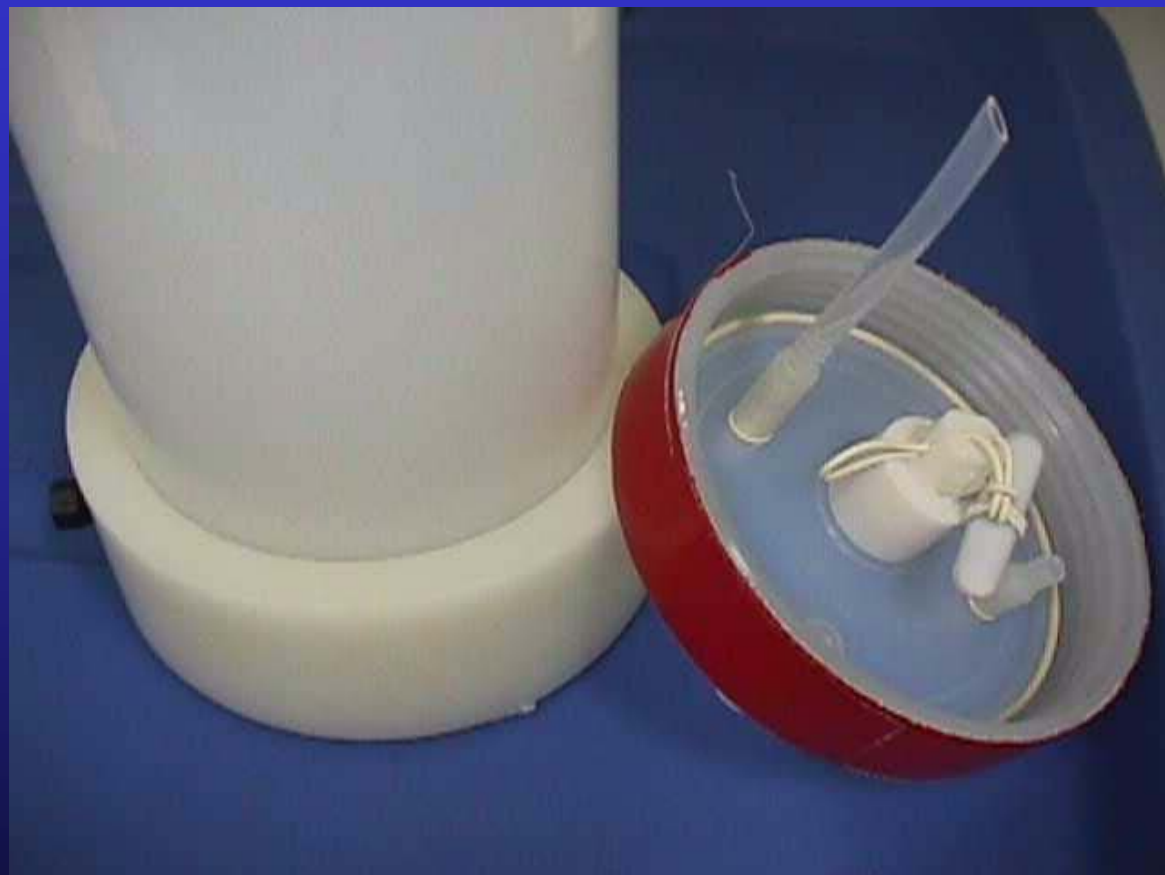


Figure 10. Benthic Macroinvertebrate Taxonomy

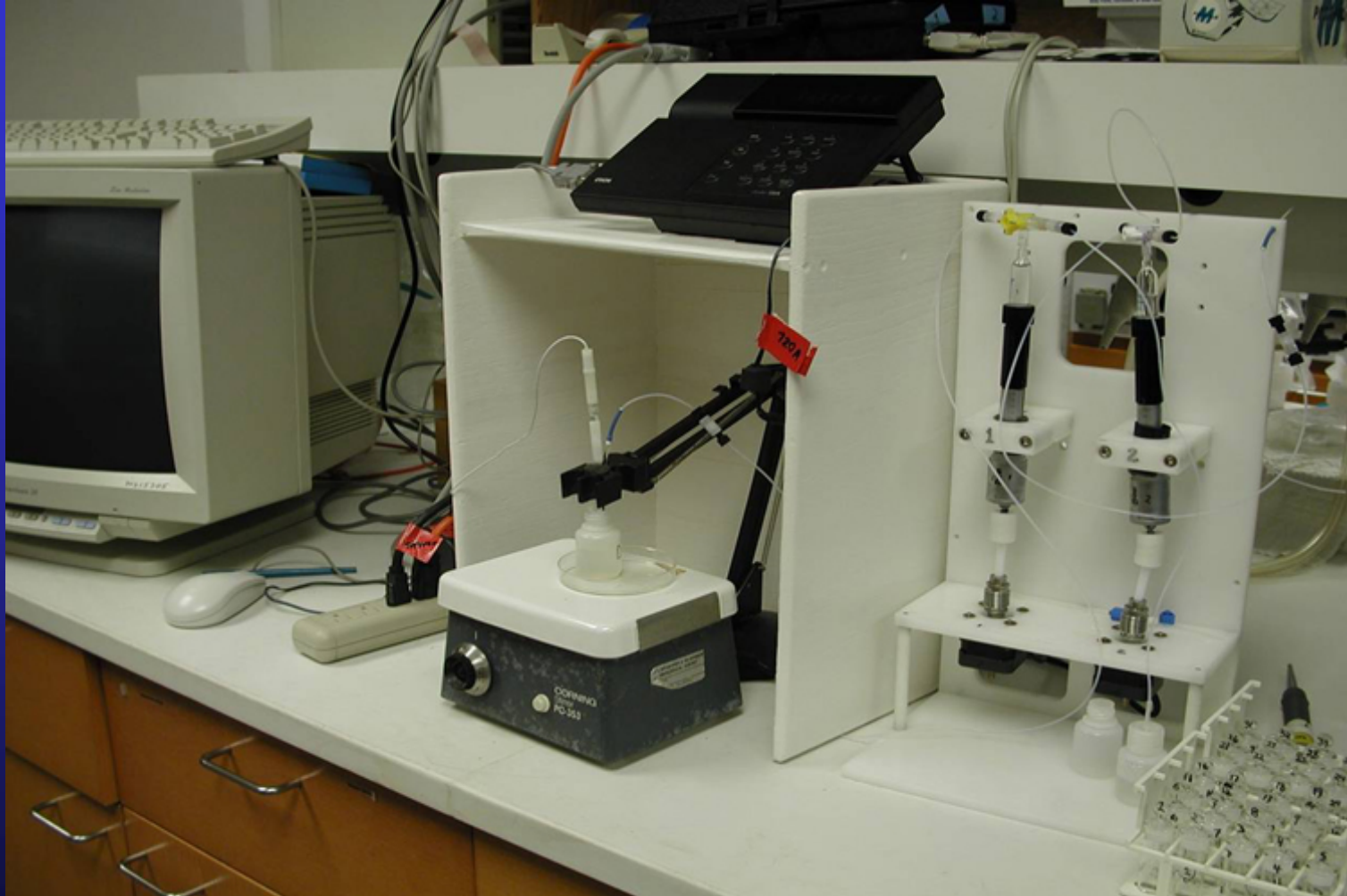


## Figure 11. Benthic Chlorophyll Analyses



Detection limit for chlorophyll analysis  
 $0.3 \text{ ug/cm}^2$

## Figure 12. Micro-Winkler Titration Method for Dissolved-Oxygen Analysis



Detection limit for dissolved-oxygen analysis  
0.5 mg/L

## Figure 13. Cold-Vapor Atomic Absorption Spectroscopy



Typical method detection limit for dissolved-mercury analysis  
0.2 pM

## Figure 14. Dissolved-Metal Analysis by ICP-MS



### Detection limit for metals analysis

Cu 0.01 ug/L

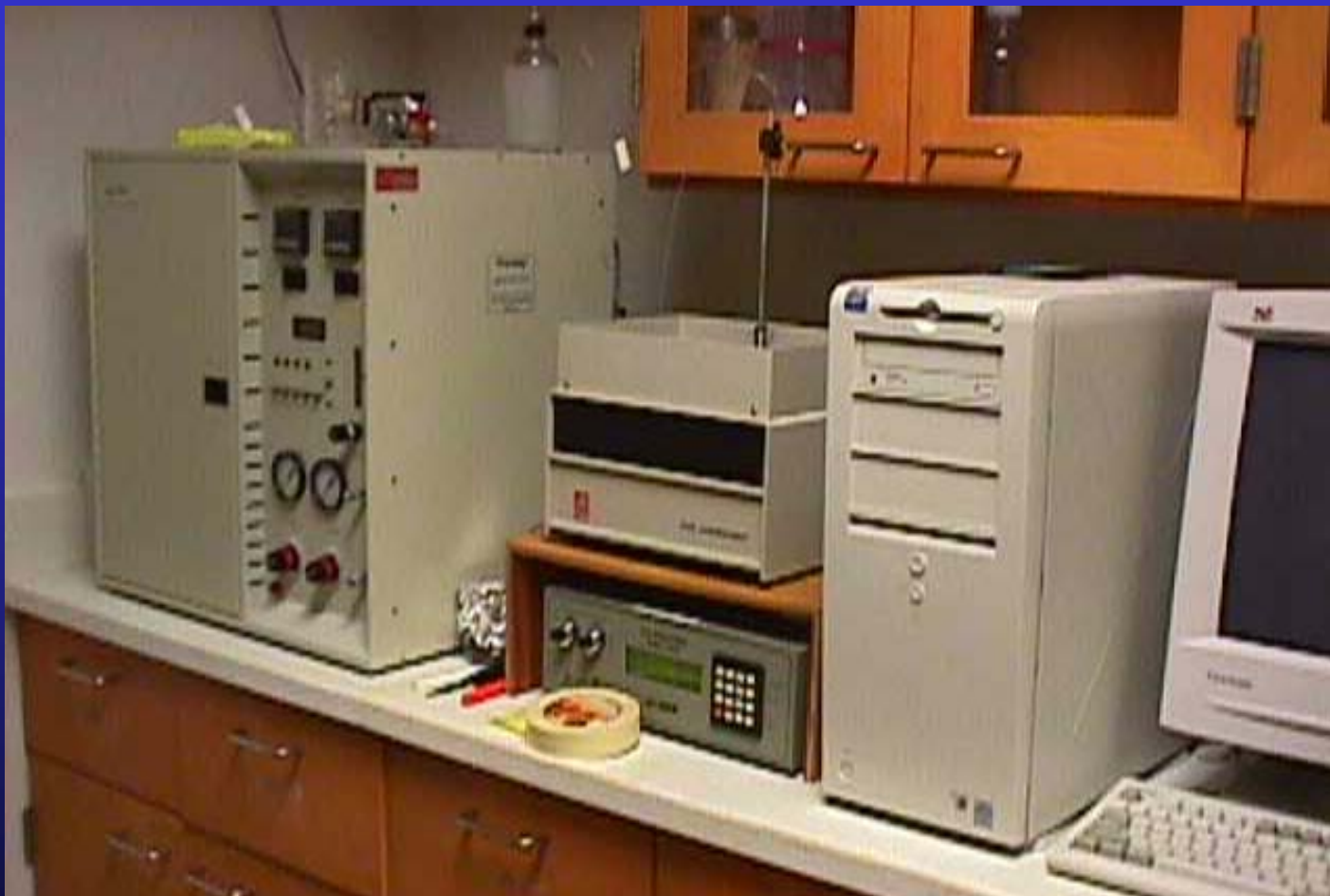
Ni 0.05 ug/L

## Figure 15. Dissolved-Nutrient Analysis by Automated Spectrophotometry



Detection limit for nutrient analysis  
Ortho-P 2.5 ug/L

## Figure 16. Dissolved Organic Carbon (DOC) Analyses by High-Temperature, Non-Catalytic Oxidation



Detection limit for DOC analysis  
0.1 mg/L

## Figure 17. Dissolved-Sulfide Analysis by Square-wave Voltammetry



Detection limit for sulfide analysis  
0.1 ug/L (4 nM)

**Table 1.** Macroinvertebrate Taxonomy

	Individuals/m <sup>2</sup>			
	May-03 Station 25	Nov-03	May-03 Station 29A	Nov-03
Phylum Mollusca Class Pelecypoda <i>Theora lubrica</i> <i>Venerupis philippinarum</i>	43	43 43	87	43
Phylum Arthropoda Class Crustacea Order Cumacea <i>Nippoleucon hinumensis</i> Order Isopoda <i>Paranthura elegans</i> Order Amphipoda Family Ampeliscidae <i>Ampelisca abdita</i> Family Corophidae <i>Corophium heteroceratum</i>	1602	43 43	260 87	87
Phylum Annelida Class Oligochaeta Tubificidae Class Polychaeta Family Capitellidae <i>Heteromastus filiformis</i> Family Cirratulidae <i>Cirriformia spirabrancha</i> Unid. Cirratulidae juvenile Family Dorvilleidae <i>Dorvillea rudolphi</i> Family Eunicidae <i>Marphysa nr. Sanguinea</i> Family Goniadidae <i>Glycinde polygnatha</i> <i>Glycinde</i> sp. SF1 <i>Glycinde</i> spp. Family Maldanidae <i>Sabaco elongatus</i> Family Phyllodocidae <i>Eumida longicornuta</i> Family Polynoidae <i>Harmothoe imbricata</i> Family Sabellidae <i>Euchone limnicola</i> Family Spionidae <i>Dipolydora socialis</i> <i>Polydora brachycephala</i> <i>Polydora cornuta (=ligni)</i> <i>Pseudopolydora paucibranchiata</i> Unid. Spionidae* Family Syllidae <i>Exogone lourei</i> <i>Sphaerosyllis</i> spp. <i>Typosyllis</i> sp. A Family Terebellidae <i>Ameana</i> sp. SF1 <i>Pista elongata</i> <i>Polycirrus</i> spp.? (damaged) Unid. Terebellidae	87 43 43 823 173 130 87 43 43 87 87	260 43 43 1688 43 130 43 43 216 87 87 43 260 173 173 43 130	476 216 87 43 87 43 173 476 43 260 173 173 43 260 173 43 87 43 43 130 43 130 43	
Misc. groups				
Phylum Cnidaria Class Anthozoa	43	216	43	130
Phylum Chordata <i>Molgula manhattensis</i>	43		173	43
Phylum Nematoda		87	693	736
Phylum Ectoprocta	X	X		X

\* Lost - not included in weight

X Present in sample but not weighed or counted

Wet weight (mean of 3 cores) (grams)	Station 25		Station 29A	
	May-03	Nov-03	May-03	Nov-03
Phylum Mollusca	0.000	0.208	0.000	0.003
Class Crustacea	0.011	0.001	0.014	0.003
Phylum Annelida	0.599	1.219	0.258	1.471
Misc. groups	0.051	0.004	0.000	0.006

Note: Mean number (n=3 cores) of individuals per square meter, based on core surface area of 77 cm<sup>2</sup>

**Table 2.** Discrete Benthic Chlorophyll and Phaeophytin Analysis

<b>May-03</b>		Individual Cores		Site Averages			
Station	Core	ChlA ug/cm <sup>2</sup>	Phaeo	ChlA ug/cm <sup>2</sup>	error	Phaeo ug/cm <sup>2</sup>	error
25	2	1.1	14.0	<b>2.5</b>	5.9	<b>11.3</b>	7.2
25	3	4.7	9.9				
25	4	1.7	9.9				
29A	5	1.4	9.1	<b>1.2</b>	0.9	<b>8.8</b>	2.7
29A	6	0.9	9.5				
29A	7	1.2	7.8				

<b>Nov-03</b>		Individual Cores		Site Averages			
Station	Core	ChlA ug/cm <sup>2</sup>	Phaeo	ChlA ug/cm <sup>2</sup>	error	Phaeo ug/cm <sup>2</sup>	error
25	5	0.5	14.5	<b>0.4</b>	0.1	<b>13.4</b>	6.7
25	7	0.5	14.8				
25	8	0.4	10.8				
29A	1	0.1	8.5	<b>0.2</b>	0.2	<b>9.0</b>	8.6
29A	2	<0.1	12.1				
29A	3	0.2	6.5				

Notes: Errors shown represent 95% confidence intervals.

**Table 3.** Water-Column Mercury Concentrations

<b>May-03</b>		
St. 25 depth	Total Dissolved Hg (pM)	
	mean	stdev
1 m	<b>10.0</b>	<b>0.2</b>
St. 29a depth		
	mean	stdev
	1 m	<b>7.0</b> <b>0.1</b>
	Mid	<b>6.8</b> <b>0.0</b>
12 m	<b>5.4</b> <b>0.5</b>	

<b>Nov-03</b>		
St. 25 depth	Total Dissolved Hg (pM)	
	mean	stdev
1 m	<b>5.7</b>	<b>0.9</b>
St. 29a depth		
	mean	stdev
	1 m	<b>4.7</b> <b>0.1</b>
	Mid	<b>3.8</b> <b>0.1</b>
12 m	<b>4.8</b> <b>0.2</b>	

**Table 4.** Benthic Flux of Total Dissolved Mercury

<b>May-03</b>							Site Averages Mercury Flux (ng/m2-day) <sup>b</sup>	Areal Averaged <sup>c</sup> Mercury Flux g/day
Sta.	Core	Mercury Flux (pmoles/m2-h) <sup>a</sup>	Mercury Flux (ng/m2-day) <sup>b</sup>	r <sup>2</sup>	n	Comments		
25	2	40 +/- 6	194 +/- 29	0.97	7		203 +/- 51	113 +/- 28
25	3	33 +/- 33	158 +/- 159	0.41	8			
25	4	54 +/- 9	258 +/- 43	0.94	8		429 +/- 497	238 +/- 275
29A	5	208 +/- 31	999 +/- 152	0.95	8	Potential outlier <sup>c</sup>		
29A	6	42 +/- 18	203 +/- 86	0.73	8			
29A	7	18 +/- 23	87 +/- 112	0.34	8			

Calculated without end points due to potentially anoxic conditions				
Sta.	Core	Mercury Flux (pmoles/m2-h) <sup>a</sup>	Mercury Flux (ng/m2-day) <sup>b</sup>	r <sup>2</sup> n
25	2	24 +/- 12	117 +/- 58	1.00 4
25	3	82 +/- 111	396 +/- 534	0.99 4
25	4	23 +/- 19	113 +/- 89	1.00 4
29A	5	83 +/- 30	401 +/- 142	1.00 4
29A	6	107 +/- 29	517 +/- 141	1.00 4
29A	7	37 +/- 82	177 +/- 396	1.00 4

All Sites/Dates Areal Averaged <sup>c</sup> Mercury Flux g/day
<b>135 +/- 94</b>

<b>Nov-03</b>							Site Averages Mercury Flux (ng/m2-day) <sup>b</sup>	Areal Averaged <sup>c</sup> Mercury Flux g/day
Sta.	Core	Mercury Flux (pmoles/m2-h) <sup>a</sup>	Mercury Flux (ng/m2-day) <sup>b</sup>	r <sup>2</sup>	n	Comments		
25	5	38 +/- 3	184 +/- 15	0.99	6		225 +/- 137	125 +/- 76
25	7	23 +/- 54	112 +/- 261	0.95	5	Final time point sample was lost		
25	8	78 +/- 1174	378 +/- 5652	0.77	3	Initial time point sample was contaminated	120 +/- 101	66 +/- 56
29A	1	6 +/- 4	29 +/- 17	0.80	6			
29A	2	21 +/- 17	102 +/- 82	0.83	5			
29A	3	47 +/- 12	228 +/- 60	0.91	7			

Notes: All methyl mercury samples were below detection limits, so no methyl mercury fluxes can be directly estimated (see [discussion](#)).  
 Errors shown for individual cores and for "all sites/dates" average represent 95% confidence intervals.  
 Errors shown for site averages and areal averages represent standard deviations of the values used in the mean.  
 r<sup>2</sup> represents the correlation coefficient of the regression of concentration versus time

<sup>a</sup> Total dissolved mercury flux (molar units) is presented in picomoles per square meter per hour.

<sup>b</sup> Total dissolved mercury flux (mass units) is presented in nanograms per square meter per day.

<sup>c</sup> Flux values were extrapolated over the entire South Bay (south of the Bay Bridge) using an area of 554 km<sup>2</sup> (Cheng and Gartner, 1985)

<sup>d</sup> The concentration of the final time point at this site was the highest of all values, so it is possibly an outlier due to contamination. If the flux is calculated without this point, the result is 83.3 +/- 25.1 pmoles/m2-h.

**Table 5.** Dissolved Sulfide Flux

<b>May-03</b>		Sulfide Flux			<b>Site Averages</b>
Sta.	Core	(nmoles/m <sup>2</sup> -h)	r <sup>2</sup>	n	Sulfide Flux (nmoles/m <sup>2</sup> -h)
25	2	<b>507</b> +/- 63	0.93	8	<b>653</b> +/- 127
25	3	<b>711</b> +/- 96	0.92	8	
25	4	<b>739</b> +/- 90	0.93	8	
29A	5	<b>708</b> +/- 32	0.99	8	<b>786</b> +/- 86
29A	6	<b>771</b> +/- 89	0.94	8	
29A	7	<b>878</b> +/- 57	0.98	8	

<b>Nov-03</b>		Sulfide Flux			<b>Site Averages</b>
Sta.	Core	(nmoles/m <sup>2</sup> -h)	r <sup>2</sup>	n	Sulfide Flux (nmoles/m <sup>2</sup> -h)
25	5	<b>466</b> +/- 41	0.96	8	<b>564</b> +/- 98
25	7	<b>563</b> +/- 57	0.95	8	
25	8	<b>662</b> +/- 44	0.98	8	
29A	1	<b>778</b> +/- 79	0.95	8	<b>751</b> +/- 72
29A	2	<b>805</b> +/- 32	0.99	8	
29A	3	<b>670</b> +/- 57	0.97	8	

Notes: Errors shown for individual cores represent 95% confidence intervals.

Errors shown for site averages represent standard deviations of the values used in the mean.

r<sup>2</sup> represents the correlation coefficient of the regression of concentration versus time

**Table 6.** Dissolved Organic Carbon Fluxes and Water-Column Concentrations in South San Francisco Bay, CA

<b>May-03</b>		DOC Flux			<b>Site Averages</b>
Core	Sta.	( $\mu\text{moles}/\text{m}^2\text{-h}$ )	$r^2$	n	DOC Flux ( $\text{nmoles}/\text{m}^2\text{-h}$ )
25	2	<b>-129</b> +/- 24	0.50	15	<b>-135</b> +/- 29
25	3	<b>-167</b> +/- 27	0.57	15	
25	4	<b>-109</b> +/- 64	0.09	15	
29A	5	<b>101</b> +/- 38	0.20	15	<b>27</b> +/- 158
29A	6	<b>134</b> +/- 35	0.38	14	
29A	7	<b>-155</b> +/- 29	0.46	16	
Water Column		DOC ( $\mu\text{M}$ )			
Sta. 25	Bottom	<b>263</b> +/- 1			
Sta. 29a	Surface	<b>215</b> +/- 3			
	Mid-depth	<b>221</b> +/- 1			
	Bottom	<b>219</b> +/- 2			
<b>Nov-03</b>		DOC Flux			<b>Site Averages</b>
Core	Sta.	( $\mu\text{moles}/\text{m}^2\text{-h}$ )	$r^2$	n	DOC Flux ( $\text{nmoles}/\text{m}^2\text{-h}$ )
25	5	<b>85</b> +/- 115	0.02	14	<b>371</b> +/- 255
25	7	<b>575</b> +/- 50	0.82	15	
25	8	<b>453</b> +/- 164	0.24	14	
29A	1	<b>1264</b> +/- 226	0.57	14	<b>1302</b> +/- 168
29A	2	<b>1156</b> +/- 232	0.51	14	
29A	3	<b>1486</b> +/- 160	0.75	15	
Water Column		DOC ( $\mu\text{M}$ )			
Sta. 25	Bottom	<b>242</b> +/- 1			
Sta. 29a	Surface	<b>156</b> +/- 2			
	Mid-depth	<b>156</b> +/- 3			
	Bottom	<b>154</b> +/- 1			

Notes: Errors shown for individual cores represent 95% confidence intervals.  
 Errors shown for site averages represent standard deviations of the values used in the mean.  
 $r^2$  represents the correlation coefficient of the regression of concentration versus time

**Table 7.** Dissolved Oxygen Flux (i.e. Consumption) in South San Francisco Bay, CA

<b>May-03</b>						<b>Site Averages</b>	
Core	DO Flux				n	DOC Flux	
	Sta.	(mmoles/m <sup>2</sup> -h)		r <sup>2</sup>		(nmoles/m <sup>2</sup> -h)	
2	25	<b>-4.4</b>	+/- 3.0	0.93	4	<b>-4.5</b>	+/- 0.4
3	25	<b>-4.3</b>	+/- 3.0	0.93	4		
4	25	<b>-5.0</b>	+/- 2.4	0.96	4		
5	29A	<b>-4.5</b>	+/- 0.4	1.00	4		
6	29A	<b>-4.8</b>	+/- 3.8	0.91	4		
7	29A	<b>-4.4</b>	+/- 1.9	0.97	4		
<b>Spring Average</b>							

<b>Nov-03</b>						<b>Site Averages</b>	
Core	DO Flux				n	DOC Flux	
	Sta.	(mmoles/m <sup>2</sup> -h)		r <sup>2</sup>		(nmoles/m <sup>2</sup> -h)	
5	25	<b>-2.5</b>	+/- 2.3	0.88	4	<b>-3.1</b>	+/- 0.6
7	25	<b>-3.2</b>	+/- 2.4	0.92	4		
8	25	<b>-3.6</b>	+/- 2.7	0.92	4		
1	29A	<b>-3.5</b>	+/- 2.1	0.95	4		
2	29A	<b>-3.2</b>	+/- 4.5	0.77	4		
3	29A	<b>-3.7</b>	+/- 1.4	0.98	4		
<b>Autumn Average</b>							

Notes: Errors shown for individual cores/ seasonal averages represent 95% confidence intervals.  
 Errors shown for site averages represent standard deviations of the values used in the mean.  
 r<sup>2</sup> represents the correlation coefficient of the regression of concentration versus time

**Table 8.** Benthic Flux and Water-column Concentrations for Dissolved Nickel and Copper

**Nickel**

May-03		Ni Flux			
Sta.	Core	(nmoles/m <sup>2</sup> -h)	r <sup>2</sup>	n	
25	2	-11 +/- 4	0.13	17	
25	3	26 +/- 4	0.49	17	
25	4	-21 +/- 9	0.21	14	
29A	5	13 +/- 4	0.22	17	
29A	6	24 +/- 4	0.52	15	
29A	7	49 +/- 6	0.67	16	
Water Column		Ni (nM)			
Sta. 25	Bottom	29.8 +/- 0.2			
Sta. 29a	Surface	25.2 +/- 0.5			
	Mid-depth	24.8 +/- 0.1			
	Bottom	24.8 +/- 0.5			

Nov-03		Ni Flux			
Sta.	Core	(nmoles/m <sup>2</sup> -h)	r <sup>2</sup>	n	
25	5	-9 +/- 9	0.05	13	
25	7	-29 +/- 7	0.46	13	
25	8	-18 +/- 12	0.10	13	
29A	1	114 +/- 5	0.96	14	
29A	2	73 +/- 4	0.92	16	
29A	3	102 +/- 5	0.94	15	
Water Column		Ni (nM)			
Sta. 25	Bottom	23.4 +/- 0.2			
Sta. 29a	Surface	22.7 +/- 1.2			
	Mid-depth	23.5 +/- 0.5			
	Bottom	22.1 +/- 0.5			

**Copper**

May-03		Cu Flux			
Sta.	Core	(nmoles/m <sup>2</sup> -h)	r <sup>2</sup>	n	
2	25	-41 +/- 12	0.37	13	
3	25	5 +/- 3	0.07	16	
4	25	-48 +/- 5	0.72	16	
5	29A	-62 +/- 4	0.91	15	
6	29A	-81 +/- 10	0.69	15	
7	29A	-19 +/- 4	0.31	18	
Water Column		Cu (nM)			
Sta. 25	Bottom	29.7 +/- 0.4			
Sta. 29a	Surface	27.1 +/- 0.1			
	Mid-depth	28.3 +/- 0.6			
	Bottom	23.7 +/- 0.2			

Nov-03		Cu Flux			
Sta.	Core	(nmoles/m <sup>2</sup> -h)	r <sup>2</sup>	n	
5	25	-9 +/- 3	0.20	16	
7	25	-3 +/- 9	0.00	16	
8	25	28 +/- 22	0.09	12	
1	29a	-82 +/- 12	0.74	12	
2	29a	-97 +/- 8	0.86	14	
3	29a	-8 +/- 2	0.22	17	
Water Column		Cu (nM)			
Sta. 25	Bottom	29.0 +/- 0.2			
Sta. 29a	Surface	25.5 +/- 0.0			
	Mid-depth	26.4 +/- 0.5			
	Bottom	25.1 +/- 0.4			

Notes: Errors shown for individual cores represent 95% confidence intervals.  
r<sup>2</sup> represents the correlation coefficient of the regression of concentration versus time

**Table 9.** Macronutrient benthic flux

<b>May-03</b>						
<b>NITRATE PLUS NITRITE</b>						
Sta.	Core	NO3 Flux (umoles/m2-h)		$r^2$	n	
25	2	-1	+/- 9	0.04	4	
25	3	-7	+/- 29	0.03	6	
25	4	-17	+/- 17	0.25	7	
29A	5	40	+/- 52	0.92	4	
29A	6	32	+/- 8	0.99	4	
29A	7	32	+/- 20	0.98	4	
<b>AMMONIA</b>						
Sta.	Core	NH4+ Flux (umoles/m2-h)		$r^2$	n	
25	2	9	+/- 2	0.98	5	
25	3	42	+/- 3	0.99	7	
25	4	47	+/- 6	0.95	7	
29A	5	17	+/- 40	0.54	4	
29A	6	12	+/- 42	0.34	4	
29A	7	11	+/- 2	0.99	4	
<b>ORTHOPHOSPHATE</b>						
Sta.	Core	PO4 Flux (umoles/m2-h)		$r^2$	n	
25	2	1	+/- 9	0.02	5	
25	3	15	+/- 16	0.31	7	
25	4	2	+/- 9	0.02	7	
29A	5	0	+/- 30	0.01	4	
29A	6	-12	+/- 16	0.79	4	
29A	7	-2	+/- 1	0.99	4	
<b>SILICA</b>						
Sta.	Core	Si Flux (umoles/m2-h)		$r^2$	n	
25	2	277	+/- 277	0.74	4	
25	3	473	+/- 187	0.76	7	
25	4	200	+/- 79	0.70	7	
29A	5	531	+/- 774	0.75	4	
29A	6	368	+/- 158	0.97	4	
29A	7	342	+/- 74	0.99	4	

<b>Nov-03</b>						
<b>NITRATE PLUS NITRITE</b>						
Sta.	Core	NO3 Flux (umoles/m2-h)		$r^2$	n	
25	5	6	+/- 8	0.65	4	
25	7	1	+/- 15	0.01	4	
25	8	30	+/- 45	0.58	4	
29A	1	-20	+/- 6	0.98	4	
29A	2	-26	+/- 9	0.96	4	
29A	3	-14	+/- 9	0.88	4	
<b>AMMONIA</b>						
Sta.	Core	NH4+ Flux (umoles/m2-h)		$r^2$	n	
25	5	-18	+/- 6	0.96	4	
25	7	-14	+/- 10	0.87	4	
25	8	9	+/- 4	0.93	4	
29A	1	23	+/- 10	0.94	4	
29A	2	-26	+/- 16	0.9	4	
29A	3	24	+/- 14	0.91	4	
<b>ORTHOPHOSPHATE</b>						
Sta.	Core	PO4 Flux (umoles/m2-h)		$r^2$	n	
25	5	9	+/- 4	0.94	4	
25	7	4	+/- 2	0.87	4	
25	8	7	+/- 3	0.93	4	
29A	1	-16	+/- 7	0.93	4	
29A	2	-8	+/- 60	0.05	4	
29A	3	-15	+/- 6	0.94	4	
<b>SILICA</b>						
Sta.	Core	Si Flux (umoles/m2-h)		$r^2$	n	
25	5	171	+/- 59	0.96	4	
25	7	193	+/- 79	0.95	4	
25	8	285	+/- 133	0.93	4	
29A	1	243	+/- 120	0.93	4	
29A	2	178	+/- 94	0.92	4	
29A	3	168	+/- 83	0.93	4	

Notes: Errors shown for individual cores represent 95% confidence intervals.

$r^2$  represents the correlation coefficient of the regression of concentration versus time

**Table 10.** Ancillary sediment characterization data

Sediment Parameter	Units	Apr-03		Nov-03		Explanation
		Sta. 25	Sta. 29A	Sta. 25	Sta. 29A	
MeHg Prod Potential dev <sup>a</sup>	ng/g dry sed/d	<b>4.1</b> 2.2	<b>7.2</b> 2.3	<b>&lt; 0.70</b>	<b>6.3</b> 0.7	Methyl-mercury production potential rate in nanograms per gram dry sediment per day
MeHg Degrad Potential dev <sup>a</sup>	ng/g dry sed/d	<b>8.7</b> 0.2	<b>7.3</b> 0.2	<b>4.0</b> 0.2	<b>4.1</b> 0.0	Methyl-mercury degradation potential rate in nanograms per gram dry sediment per day
M/D Ratio	unitless	<b>0.47</b>	<b>0.98</b>	<b>&lt; 0.18</b>	<b>1.54</b>	Production(methylation)/degradation(demethylation) ratio
Microbial Sulfate Red. dev <sup>a</sup>	nmol/g dry sed/d	<b>7.8</b> 2.4	<b>4.8</b> 2.3	<b>1.6</b> 0.0	<b>1.4</b> 0.0	Microbial sulfate reduction rate in nanomoles per gram dry sediment per day
Total Hg dev <sup>a</sup>	ng/g dry sed	<b>256</b> 9	<b>293</b> 33	<b>233</b> 4	<b>247</b> 5	Total mercury concentration in sediment in micrograms per gram dry sediment
Reactive Hg(II) dev <sup>a</sup>	ng/g dry sed	<b>1.41</b> 0.97	<b>1.96</b> 0.29	<b>1.24</b> 0.46	<b>0.38</b> 0.01	Reactive mercury in sediment, operationally defined as the SnCl <sub>2</sub> reducible Hg(II), in nanomoles per gram dry sediment
Percent Reactive Hg(II) dev <sup>a</sup>	%	<b>0.55</b> 0.38	<b>0.67</b> 0.10	<b>0.53</b> 0.20	<b>0.16</b> 0.00	Percent of total Hg recovered as reactive Hg(II)
Loss on Ignition dev <sup>a</sup>	%	<b>5.83</b> 0.3	<b>6.08</b> 0.3	<b>4.32</b> 1.1	<b>4.75</b> 0.2	Loss of organics on heat application
Acid Volatile Sulfur dev <sup>a</sup>	umol/g dry sed	<b>1.9</b> 1.0	<b>17.0</b> 2.7	<b>10.5</b> 0.0	<b>33.4</b> 0.0	Acid volatile sulfur concentration in micromoles per gram dry sediment
Total Reduced Sulfur dev <sup>a</sup>	umol/g dry sed	<b>72.4</b> 1.8	<b>64.7</b> 5.9	<b>69.5</b> 0.0	<b>172.8</b> 0.4	Total reduced sulfur concentration in micromoles per gram dry sediment
Sediment Fe(II) dev <sup>a</sup>	mg/g dry sed	<b>5.14</b> 0.03	<b>8.49</b> 0.04	<b>9.09</b> 0.11	<b>11.46</b> 1.12	Concentration of iron in oxidation state (II) in milligrams per gram dry sediment
Amorphous Fe(III) dev <sup>a</sup>	mg/g dry sed	<b>2.95</b> 0.10	<b>0.05</b> 0.01	<b>0.35</b> 0.10	<b>-0.48</b> 0.41	Concentration of amorphous iron in oxidation state (III) in milligrams per gram dry sediment
Crystalline Fe(III) dev <sup>a</sup>	mg/g dry sed	<b>2.15</b> 0.52	<b>1.18</b> 0.20	<b>7.02</b> 0.26	<b>3.10</b> 0.72	Concentration of crystalline iron in oxidation state (III) in milligrams per gram dry sediment
Fe(II)/Fe ratio	%	<b>50.2</b>	<b>87.3</b>	<b>55.2</b>	<b>81.4</b>	Percent of total iron as Fe(II)
Porewater Fe(II) dev <sup>a</sup>	mg/liter	<b>0.03</b> (n=1)	<b>0.50</b> 0.05	<b>0.02</b> (n=1)	<b>1.32</b> (n=1)	Porewater concentration of Fe(II) in milligrams per liter of porewater
Porewater Sulfate dev <sup>a</sup>	mM	<b>19.8</b> 0.9	<b>19.3</b> 1.0	<b>20.0</b> (n=1)	<b>18.8</b> (n=1)	Porewater concentration of sulfate in millimoles per liter of porewater
Porewater Chloride dev <sup>a</sup>	mM	<b>443</b> 6	<b>444</b> 14	<b>438</b> (n=1)	<b>451</b> (n=1)	Porewater concentration of chloride in millimoles per liter of porewater
Sulfate/Chloride ratio	unitless	<b>0.04</b>	<b>0.04</b>	<b>0.05</b>	<b>0.04</b>	Molar concentration ratio in porewater
Porewater Sulfide dev <sup>a</sup>	uM	<b>&lt; 0.2</b>	<b>0.58</b> 0.09	<b>&lt; 0.2</b>	<b>&lt; 0.2</b>	Porewater concentration of sulfide in micromoles per liter of porewater
Porewater DOC dev <sup>a</sup>	mg-C/L	<b>37.5</b> 2.0	<b>35.2</b> 0.5	<b>62.1</b> (n=1)	<b>86.7</b> (n=1)	Porewater concentration of dissolved organic carbon in milligrams of carbon per liter of porewater
Sediment Eh redox (n=1)	mV	<b>171.8</b>	<b>63.5</b>	<b>71.6</b>	<b>38.7</b>	Reducing potential at time of incubation

<sup>a</sup> All deviations (dev) are based on two replicates (n=2) unless otherwise indicated